Jamieson ER, Lippard SJ (1999) Structure, recognition, and processing of cisplatin-DNA adducts. *Chem Rev* **99:** 2467–2498

Kirouac KN, Ling H (2009) Structural basis of error-prone replication and stalling at a thymine base by human DNA polymerase iota. *EMBO J* **28:** 1644–1654

Kraut DA, Sigala PA, Pybus B, Liu CW, Ringe D, Petsko GA, Herschlag D (2006) Testing electrostatic complementarity in enzyme catalysis: hydrogen bonding in the ketosteroid isomerase oxyanion hole. *PLoS Biol* **4:** e99

Lehmann AR (2002) Replication of damaged DNA in mammalian cells: new solutions to an old problem. *Mutat Res* **509:** 23–34

Ling H, Boudsocq F, Plosky BS, Woodgate R, Yang W (2003) Replication of a cis-syn thymine dimer at atomic resolution. *Nature* **424:** 1083–1087

Ling H, Boudsocq F, Woodgate R, Yang W (2001) Crystal structure of a Y-family DNA polymerase in action: a mechanism for error-prone and lesion-bypass replication. *Cell* **107:** 91–102

Ling H, Boudsocq F, Woodgate R, Yang W (2004a) Snapshots of replication through an abasic lesion; structural basis for base substitutions and frameshifts. *Mol Cell* **13:** 751–762

Ling H, Sayer JM, Plosky BS, Yagi H, Boudsocq F, Woodgate R, Jerina DM, Yang W (2004b) Crystal structure of a benzo[a]pyrene diol epoxide adduct in a ternary complex with a DNA polymerase. *Proc Natl Acad Sci USA* **101:** 2265–2269

Lippert B (1999) *Cisplatin: Chemistry and Biochemistry of a Leading Anticancer Drug*. Zürich: Helvetica Chimica

Lone S, Townson SA, Uljon SN, Johnson RE, Brahma A, Nair DT, Prakash S, Prakash L, Aggarwal AK (2007) Human DNA polymerase kappa encircles DNA: implications for mismatch extension and lesion bypass. *Mol Cell* **25:** 601–614

Mamenta EL, Poma EE, Kaufmann WK, Delmastro DA, Grady HL, Chaney SG (1994) Enhanced replicative bypass of platinum-DNA adducts in cisplatin-resistant human ovarian carcinoma cell lines. *Cancer Res* **54:** 3500–3505

McCoy AJ, Grosse-Kunstleve RW, Storoni LC, Read RJ (2005) Likelihood-enhanced fast translation functions. *Acta Crystallogr D Biol Crystallogr* **61:** 458–464

McCulloch SD, Kunkel TA (2008) The fidelity of DNA synthesis by eukaryotic replicative and translesion synthesis polymerases. *Cell Res* **18:** 148–161

Nair DT, Johnson RE, Prakash L, Prakash S, Aggarwal AK (2006) An incoming nucleotide imposes an anti to syn conformational change on the templating purine in the human DNA polymerase-iota active site. *Structure* **14:** 749–755

Ohndorf UM, Rould MA, He Q, Pabo CO, Lippard SJ (1999) Basis for recognition of cisplatin-modified DNA by high-mobility-group proteins. *Nature* **399:** 708–712

Otwinowski Z, Minor W (1997) Processing of X-ray diffraction data collected in oscillation mode. *Methods Enzymol* **276:** 307–326

Pinto AL, Lippard SJ (1985) Binding of the antitumor drug cis-diamminedichloroplatinum(II) (cisplatin) to DNA. *Biochim Biophys Acta* **780:** 167–180

Rabik CA, Dolan ME (2007) Molecular mechanisms of resistance and toxicity associated with platinating agents. *Cancer Treat Rev* **33:** 9–23

Rechkoblit O, Malinina L, Cheng Y, Kuryavyi V, Broyde S, Geacintov NE, Patel DJ (2006) Stepwise translocation of Dpo4 polymerase during error-free bypass of an oxoG lesion. *PLoS Biol* **4:** e11

Richon VM, Schulte N, Eastman A (1987) Multiple mechanisms of resistance to cis-diamminedichloroplatinum(II) in murine leukemia L1210 cells. *Cancer Res* **47:** 2056–2061

Rockabrand D, Livers K, Austin T, Kaiser R, Jensen D, Burgess R, Blum P (1998) Roles of DnaK and RpoS in starvation-induced thermotolerance of Escherichia coli. *J Bacteriol* **180:** 846–854

Rolfsmeier M, Haseltine C, Bini E, Clark A, Blum P (1998) Molecular characterization of the alpha-glucosidase gene (malA) from the hyperthermophilic archaeon Sulfolobus solfataricus. *J Bacteriol* **180:** 1287–1295

Roush AA, Suarez M, Friedberg EC, Radman M, Siede W (1998) Deletion of the Saccharomyces cerevisiae gene RAD30 encoding an Escherichia coli DinB homolog confers UV radiation sensitivity and altered mutability. *Mol Gen Genet* **257:** 686–692

Schelert J, Dixit V, Hoang V, Simbahan J, Drozda M, Blum P (2004) Occurrence and characterization of mercury resistance in the hyperthermophilic archaeon Sulfolobus solfataricus by use of gene disruption. *J Bacteriol* **186:** 427–437

Shachar S, Ziv O, Avkin S, Adar S, Wittschieben J, Reissner T, Chaney S, Friedberg EC, Wang Z, Carell T, Geacintov N, Livneh Z (2009) Two-polymerase mechanisms dictate error-free and error-prone translesion DNA synthesis in mammals. *EMBO J* **28:** 383–393

Sherman SE, Gibson D, Wang AH, Lippard SJ (1985) X-ray structure of the major adduct of the anticancer drug cisplatin with DNA: cis-[Pt(NH3)2(d(pGpG))]. *Science* **230:** 412–417

Siddik ZH (2003) Cisplatin: mode of cytotoxic action and molecular basis of resistance. *Oncogene* **22:** 7265–7279

Suo Z, Lippard SJ, Johnson KA (1999) Single d(GpG)/cis-diammineplatinum(II) adduct-induced inhibition of DNA polymerization. *Biochemistry* **38:** 715–726

Takahara PM, Rosenzweig AC, Frederick CA, Lippard SJ (1995) Crystal structure of double-stranded DNA containing the major adduct of the anticancer drug cisplatin. *Nature* **377:** 649–652

Vaisman A, Chaney SG (2000) The efficiency and fidelity of translesion synthesis past cisplatin and oxaliplatin GpG adducts by human DNA polymerase beta. *J Biol Chem* **275:** 13017–13025

Vaisman A, Ling H, Woodgate R, Yang W (2005) Fidelity of Dpo4: effect of metal ions, nucleotide selection and pyrophosphorolysis. *EMBO J* **24:** 2957–2967

Vaisman A, Masutani C, Hanaoka F, Chaney SG (2000) Efficient translesion replication past oxaliplatin and cisplatin GpG adducts by human DNA polymerase eta. *Biochemistry* **39:** 4575–4580

Vaisman A, Varchenko M, Umar A, Kunkel TA, Risinger JI, Barrett JC, Hamilton TC, Chaney SG (1998) The role of hMLH1, hMSH3, and hMSH6 defects in cisplatin and oxaliplatin resistance: correlation with replicative bypass of platinum-DNA adducts. *Cancer Res* **58:** 3579–3585

Wong JH, Fiala KA, Suo Z, Ling H (2008) Snapshots of a Y-family DNA polymerase in replication: substrate-induced conformational transitions and implications for fidelity of Dpo4. *J Mol Biol* **379:** 317–330

Worthington P, Hoang V, Perez-Pomares F, Blum P (2003) Targeted disruption of the alpha-amylase gene in the hyperthermophilic archaeon Sulfolobus solfataricus. *J Bacteriol* **185:** 482–488

Wu B, Droge P, Davey CA (2008) Site selectivity of platinum anticancer therapeutics. *Nat Chem Biol* **4:** 110–112

Yang W, Woodgate R (2007) What a difference a decade makes: insights into translesion DNA synthesis. *Proc Natl Acad Sci USA* **104:** 15591–15598

Yao S, Plastaras J, Marzilli LG (1994) A molecular mechanics AMBER-type force field for modeling platinum complexes of guanine derivatives. *Inorg Chem* **33:** 6061–6077

Zorbas H, Keppler BK (2005) Cisplatin damage: are DNA repair proteins saviors or traitors to the cell? *Chembiochem* **6:** 1157–1166

TOXICOLOGICAL SCIENCES 114(1), 71–78 (2010)
doi:10.1093/toxsci/kfp306
Advance Access publication December 21, 2009

Integration of *In Vivo* Genotoxicity and Short-term Carcinogenicity Assays Using F344 *gpt* Delta Transgenic Rats: *In Vivo* Mutagenicity of 2,4-Diaminotoluene and 2,6-Diaminotoluene Structural Isomers

Naomi Toyoda-Hokaiwado,*[,2] Tomoki Inoue,†[,2] Kenichi Masumura,* Hiroyuki Hayashi,‡ Yuji Kawamura,‡ Yasushi Kurata,‡ Makiko Takamune,* Masami Yamada,* Hisakazu Sanada,§ Takashi Umemura,† Akiyoshi Nishikawa,† and Takehiko Nohmi*[,1]

**Division of Genetics and Mutagenesis and †Division of Pathology, National Institute of Health Sciences, Setagaya-ku, Tokyo 158-8501, Japan; ‡Meiji Seika Kaisha, Ltd, Kohoku-ku, Yokohama, Kanagawa 222-8567, Japan; and §Safety Research Department, Central Research Laboratories, Kaken Pharmaceutical Co., Ltd, Fujieda, Shizuoka 426-8646, Japan*

[1] To whom correspondence should be addressed at Division of Genetics and Mutagenesis, 1-18-1 Kamiyoga, Setagaya-ku, Tokyo 158-8501, Japan. Fax: +81-3-3700-2348. E-mail: nohmi@nihs.go.jp.
[2] These authors contributed to this work equally.

Received October 16, 2009; accepted December 15, 2009

An important trend in current toxicology is the replacement, reduction, and refinement of the use of experimental animals (the 3R principle). We propose a model in which *in vivo* genotoxicity and short-term carcinogenicity assays are integrated with F344 *gpt* delta transgenic rats. Using this model, the genotoxicity of chemicals can be identified in target organs using a shuttle vector λ EG10 that carries reporter genes for mutations; short-term carcinogenicity is determined by the formation of glutathione *S*-transferase placenta form (GST-P) foci in the liver. To begin validating this system, we examined the genotoxicity and hepatotoxicity of structural isomers of 2,4-diaminotoluene (2,4-DAT) and 2,6-diaminotoluene (2,6-DAT). Although both compounds are genotoxic in the Ames/*Salmonella* assay, only 2,4-DAT induces tumors in rat livers. Male F344 *gpt* delta rats were fed diet containing 2,4-DAT at doses of 125, 250, or 500 ppm for 13 weeks or 2,6-DAT at a dose of 500 ppm for the same period. The mutation frequencies of base substitutions, mainly at G:C base pairs, were significantly increased in the livers of 2,4-DAT–treated rats at all three doses. In contrast, virtually no induction of genotoxicity was identified in the kidneys of 2,4-DAT–treated rats or in the livers of 2,6-DAT–treated rats. GST-P–positive foci were detected in the livers of rats treated with 2,4-DAT at a dose of 500 ppm but not in those treated with 2,6-DAT. Integrated genotoxicity and short-term carcinogenicity assays may be useful for early identifying genotoxic and nongenotoxic carcinogens in a reduced number of experimental animals.

Key Words: ***gpt* delta transgenic rat; diaminotoluenes; genotoxicity; carcinogenicity; 3R principle.**

Transgenic rodent models have advanced the field of *in vivo* genotoxicity studies (Nohmi and Masumura, 2005; Nohmi *et al.*, 2000). In these models, λ phage DNA carrying reporter genes for mutations are integrated into the chromosomes of transgenic rodents; the phage DNA is retrieved in phage particles by *in vitro* packaging reactions. The rescued phages are introduced into *Escherichia coli* cells, and mutants that were generated in the rodents are selected. With the shuttle vector system, one can examine the mutagenicity of chemicals in any rodent organ or tissues, including germ cells (Eastmond *et al.*, 2009; Hashimoto *et al.*, 2009). In addition, the mutants recovered from the rodents can be characterized by DNA sequencing (Heddle *et al.*, 2000). Transgenic genotoxicity assays are a reliable method for determining whether genotoxicity is involved in chemical carcinogenicity in the target organs of rodents (Thybaud *et al.*, 2003).

In 1996, we developed the novel transgenic mouse *gpt* delta for *in vivo* genotoxicity assays (Nohmi *et al.*, 1996). These mice have approximately 80 copies of λ EG10 DNA at a single site in chromosome 17 of C57 BL/6J mice (Masumura *et al.*, 1999). A feature of this transgenic mouse is that two mutant selections can be performed instead of just one, to identify a wider spectrum of *in vivo* mutations: *gpt* selection to identify point mutations such as base substitutions and frameshift mutations and Spi^- selection to identify deletion mutations. Because of their sensitivity to deletion-type mutations, *gpt* delta mice have been utilized for radiation biology, cancer research, and regulatory toxicology (Aoki *et al.*, 2007; Masumura *et al.*, 2002; Shibata *et al.*, 2009; Xu *et al.*, 2007). In 2003, we established *gpt* delta rats in a Sprague-Dawley (SD) background by introducing λ EG10 DNA into fertilized SD rat eggs (Hayashi *et al.*, 2003). This *gpt* delta rat carries approximately five copies of λ EG10 DNA at a single site in chromosome 4 and is sensitive to induction of point mutations and deletions by benzo[*a*]pyrene and potassium bromate (Hayashi *et al.*, 2003; Umemura *et al.*, 2009).

Here, we report the establishment of *gpt* delta rat in a Fischer 344 background by backcross of SD *gpt* delta rats with F344 rats for 15 generations. We generated F344 *gpt* delta rats because this background is frequently used for 2-year cancer bioassays. In addition, glutathione *S*-transferase placenta form (GST-P)–positive preneoplastic hepatic foci can be analyzed in the rats (Ito *et al.*, 2000). The results of bioassay using GST-P–positive foci show good correlation with those of 2-year cancer bioassay (Ito *et al.*, 2000; Ogiso *et al.*, 1985). Therefore, GST-P–positive foci formation assay was used as short-term carcinogenicity assay in this study. We hypothesized that we could integrate a genotoxicity assay with a short-term carcinogenicity assay utilizing GST-P foci in F344 *gpt* delta rats. This would reduce the number of animals required for both assays and would allow for examination of the relationship between genotoxicity and preneoplastic lesion formation within the same organs and tissues of chemically treated F344 *gpt* delta rats.

To begin validating this system, we examined the *in vivo* genotoxicity and hepatotoxicity of 2,4-diaminotoluene (2,4-DAT) and 2,6-diaminotoluene (2,6-DAT). The first chemical, 2,4-DAT, is used as an intermediate of the production of toluene diisocyanate, which is a monomer for the production of polyurethane, while 2,6-DAT is an intermediate of dyes, rubber chemicals, and various polymers (NTP 1979, 1980). Although both are genotoxic *in vitro* (Cunningham *et al.*, 1989), only 2,4-DAT is carcinogenic in the livers of female mice and male and female rats (NTP, 1979). 2,4-DAT also induces lymphoma in female mice and mammary and subcutaneous tumors in rats. 2,6-DAT is not carcinogenic in mice and rats, regardless of their sex (NTP, 1980). Previous studies with MutaMouse (Kirkland and Beevers, 2006) and Big Blue mouse (Cunningham *et al.*, 1996) indicate that 2,4-DAT is mutagenic in the liver, while 2,6-DAT is not. However, the transgenic mice employed for these studies were males, in which the hepatocarcinogenicity of 2,4-DAT is not observed. In addition, there are no reports on *in vivo* gene mutations in rats. Thus, we decided to examine the *in vivo* genotoxicity of both compounds in the liver, as carcinogenic target organ of 2,4-DAT, and kidney, as non-carcinogenic target, along with immunohistochemical analyses. We chose 500 ppm as the highest dose for both DATs according to the dose used in the National Toxicology Program 2-year cancer bioassay (NTP, 1979, 1980). We treated the rats with chemicals for 13 weeks because this period is customarily used to determine the appropriate doses for 2-year cancer bioassays; furthermore, shorter term treatments (e.g., treatments with potassium bromate for 5 weeks [Umemura *et al.*, 2006]), sometimes do not induce detectable mutations *in vivo*.

MATERIALS AND METHODS

Establishment of F344 gpt delta rats. All the animals were maintained at Japan SLC (Shizuoka, Japan). The F344 *gpt* delta transgenic rat strain was developed by backcrosses of the original SD *gpt* delta transgenic rat with wild-type F344 rats. In brief, male SD *gpt* delta transgenic rat was mated with F344 female rat to produce an F1 generation. Offspring from the F1 generation were mated with F344 rats to yield an F2 generation. All offspring from successive backcrosses were examined for the possession of the *gpt* gene by PCR (Hayashi *et al.*, 2003). After 15 successive backcrosses, identity of the resulting rats to F344 recipient is more than 99.9%. Thus, they were referred to as F344 *gpt* delta rats.

Chemicals. 2,4-DAT (purity 95%) and 2,6-DAT (purity 98%) were purchased from Wako Pure Chemical Industries (Osaka, Japan). Diethylnitrosamine (DEN) was obtained from Sigma-Aldrich Japan (Tokyo, Japan).

Bacterial reverse mutation test (Ames test). The mutagenic activities of 2,4-DAT and 2,6-DAT were assayed in a bacterial reverse mutation assay using *Salmonella typhimurium* tester strains TA98 and YG1024, an *O*-acetyltransferase (OAT)–overexpressing derivative. The test was conducted by the preincubation method (Maron and Ames, 1983) in the presence or the absence of S9 mix. At least two plates were used for each dose, and the mean values of the number of revertants per plate were calculated. Chemicals were dissolved in dimethyl sulfoxide, which was used as the negative control.

Animals, diet, and housing conditions. Male 6-week-old F344 *gpt* delta transgenic rats were obtained from Japan SLC and housed five animals per polycarbonate cage under specific pathogen-free standard laboratory conditions: room temperature, 23°C ± 2°C; relative humidity, 60 ± 5%; with a 12:12-h light-dark cycle; and free access to CRF-1 basal diet (Oriental Yeast Company, Tokyo, Japan) and tap water. After a 1-week acclimation period, the animals were used for the experiments.

Treatments of animals. The protocol for this study was approved by the Animal Care and Utilization Committee of the National Institute of Health Sciences. Thirty male F344 *gpt* delta rats were randomized by weight into six groups. 2,4-DAT and 2,6-DAT were each mixed into Oriental CRF-1 powdered basal diet (Oriental Yeast Company) and stored at 4°C in the dark before use. Starting at 7 weeks of age, the rats were fed diets containing 0, 125, 250, or 500 ppm 2,4-DAT or 500 ppm 2,6-DAT for 13 weeks. There was also a positive control group; these rats were received a once-a-week ip injection of 20 mg/kg body weight DEN for 13 weeks. Parameters monitored included clinical signs, body weight, and food intake. The highest dose of 2,4-DAT was reduced from 500 to 400 ppm at week 9 because the dose at 500 ppm reduced the body weight of rats at week 8. All the surviving animals were killed under ether anesthesia at the end of the experiments. The liver and kidneys were isolated from each animal and were immediately excised, weighed, and cut into 2- to 3-mm-thick slices. The slices were fixed in 10% buffered formalin solution and routinely processed to paraffin blocks for histopathological examination as well as immunohistochemistry. Hematoxylin and eosin-stained tissue preparations cut from the blocks were examined by light microscopy.

Micronucleus assay. At autopsy, 60 µl of peripheral blood was obtained from the tail veins of all animals. The samples were processed according to the instructions supplied with the MicroFlow^{PLUS} kit (Litron, Rochester, NY), fixed in ultra-cold methanol, and stored immediately after fixation at −80°C until flow cytometry analysis was performed. Approximately 20,000 reticulocytes were counted for each sample using Becton-Dickinson FACSCalibur flow cytometer (Franslin Lakes, NJ) to detect the presence of micronuclei (MNs).

Immunohistochemical procedures. Liver sections of 3-µm thickness were treated with rabbit anti-rat GST-P antibody (1:1000; Medical & Biological Laboratories, Nagoya, Japan) and monoclonal mouse anti-Ki67 (MIB-5) antibody (1:50; Dako, Tokyo, Japan) (1:50), respectively. Areas and numbers of GST-P–positive foci larger than 0.1 mm in diameter of the liver sections were quantitatively measured with an image processor for analytical pathology (IPAP-WIN; Sumika Technos Company, Osaka, Japan). To investigate proliferative activity, we counted at least 1000 hepatocyte nuclei in each liver; labeling indices were calculated as the percentage of cells positive for Ki67

staining. The remaining tissues were immediately frozen in liquid nitrogen and stored at −80°C for subsequent mutation assays.

DNA isolation and in vitro packaging of λ phage DNA. High–molecular-weight genomic DNA was extracted from the liver and kidneys using the RecoverEase DNA Isolation kit (Stratagene, La Jolla, CA). λ EG10 phages were rescued using Transpack Packaging Extract (Stratagene).

gpt Mutation assay. The assay was conducted according to previously published methods (Nohmi *et al.*, 1996). All the confirmed *gpt* mutants recovered from the livers were sequenced; identical mutations from the same rat were counted as one mutant. The mutant frequencies of the *gpt* gene (*gpt* MFs) in the liver and kidney were calculated by dividing the number of confirmed 6-thioguanine–resistant colonies by the number of rescued plasmids. DNA sequencing of the *gpt* gene was performed with the BigDye Terminater Cycle Sequencing Ready Reaction (Applied Biosystems, Foster City, CA) on an ABI PRISM 310 Genetic Analyzer (Applied Biosystems).

Spi⁻ assay. The Spi⁻ assay was conducted according to previously published methods (Masumura *et al.*, 2002). To confirm the Spi⁻ phenotype of the candidates, suspensions were spotted on three types of plates on which XL-1 Blue MRA, XL-1 Blue MRA P2, or WL95 P2 strains were spread with soft agar. True Spi⁻ mutants, which made clear plaques on all of the plates, were counted. Spi⁻ mutant lysates were obtained by infecting *E. coli* LE392 with the recovered Spi⁻ mutants. The lysates were used as templates for PCR and sequencing analysis to determine the deleted regions (Masumura *et al.*, 2002). The Spi⁻ mutants were categorized into three classes: one base pair (bp) deletions, deletions of more than 1 bp, and complex mutations. The entire sequence of λ EG10 is available at http://dgm2alpha.nihs.go.jp/default.htm.

Statistical analysis. The statistical significance of the difference in the value of MFs between treated groups and negative controls was analyzed by Student's *t*-test. A p value less than 0.05 denoted the presence of a statistically significant difference. Variances in values for body weight, organ weight, and immunohistochemical data were examined by one-way ANOVA with Dunnett's multiple test to compare the differences between control and treated groups.

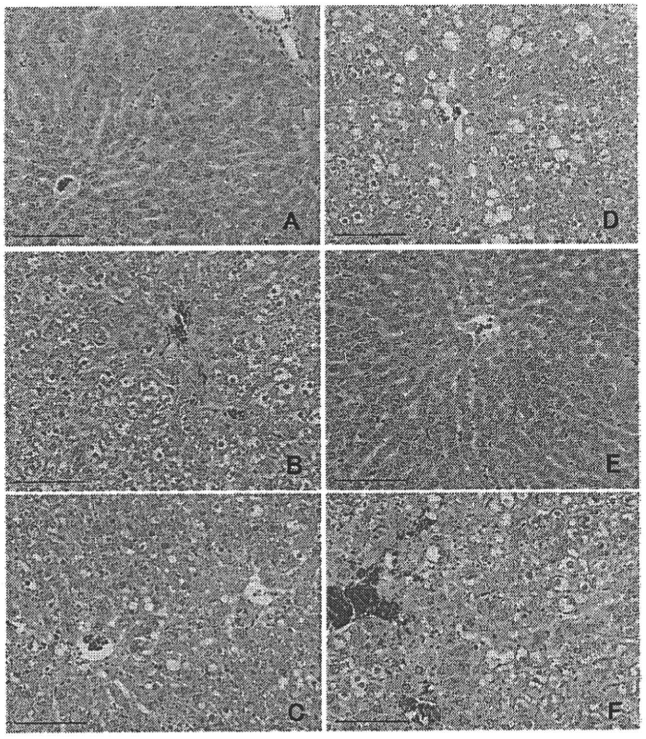

FIG. 1. Histological comparison of rat livers treated with 0 ppm 2,4-DAT (A), 125 ppm 2,4-DAT (B), 250 ppm 2,4-DAT (C), 500 ppm 2,4-DAT (D), 500 ppm 2,6-DAT (E), and DEN (F). Hepatotoxicity was observed in rats administered 2,4-DAT and DEN. Bar = 100 μm.

RESULTS

Dietary Treatment with 2,4-DAT Induced Preneoplastic Lesions in the Livers of F344 gpt Delta Rats

Dietary treatment with 2,4-DAT reduced body weight significantly at all three doses, while dietary treatment with 2,6-DAT did not (Supplementary table 1). Treatments with 2,4-DAT, but not 2,6-DAT, increased the relative weight of the livers and kidneys in a dose-dependent manner. Hypertrophy and vacuolar degeneration of hepatocytes was observed in the livers of rats in the 2,4-DAT treatment groups (Fig. 1). Cell proliferation was significantly enhanced by 2,4-DAT at a dose of 250 ppm but not by treatment with 2,6-DAT or other doses of 2,4-DAT (Table 1). That labeling index was twofold higher compared with that of basal diet group. GST-P–positive foci were induced by treatment with 2,4-DAT at a dose of 250 or 500 ppm and by the positive control treatment with DEN (Table 2). There were significant differences in number of foci and area of foci between rats treated with 2,4-DAT at 500 ppm and those of the basal diet group and between rats treated with DEN and the control group. No histopathological changes were observed in the kidneys of rats that were fed 2,4-DAT or 2,6-DAT. These results suggest that 2,4-DAT, but not 2,6-DAT, induced preneoplastic lesions in the livers of F344 *gpt* delta rats.

Both 2,4-DAT and 2,6-DAT Induced Mutations In Vitro

We confirmed that both 2,4-DAT and 2,6-DAT were mutagenic in *S. typhimurium* strain TA98 in the presence of S9 activation (Fig. 2). Treating cells with either of the DATs in the absence of S9 mix did not produce any increase in the number of revertants per plate. Similar, but less significant, results were obtained with another standard *S. typhimurium* strain TA100 (Supplementary table 2). These observations suggest that DAT metabolites were responsible for the mutagenic effects. To explore the metabolic activation pathways *in vitro*, we employed strain YG1024, which overproduces OAT, a phase II enzyme. Strain YG1024 detects frameshift mutations because it was derived from strain TA98 (Watanabe *et al.*, 1994). As shown in Figure 2, YG1024 exhibited enhanced sensitivity to the mutagenicity of both 2,4-DAT and 2,6-DAT in the presence of S9 activation. The mutagenicity of 2,6-DAT was similar to that of 2,4-DAT in the presence of S9 activation (in strain TA98, 1036 vs. 1316 His^+ revertants per plate at 625 μg of 2,4-DAT and 2,6-DAT, respectively; in strain YG1024, 3460 vs. 3896 His^+ revertants per plate at 156 μg of 2,4-DAT and 2,6-DAT, respectively).

TABLE 1
Quantification of Hepatocyte Proliferation

	No. of Rats	No. of Total Nuclei	No. of Ki-67–Positive Nuclei	Index
Basal diet	5	2170.8 ± 890.9	27.4 ± 8.1	0.013 ± 0.004
Basal diet (DEN)	5	1749.6 ± 729.2[a]	73.8 ± 19.7	0.042 ± 0.009*
125 ppm 2,4-DAT	5	1700.2 ± 700.1[a]	14.0 ± 6.6	0.008 ± 0.005
250 ppm 2,4-DAT	5	1436.4 ± 596.7[a]	44.4 ± 10.5	0.031 ± 0.007*
500 ppm 2,4-DAT	5	1308.6 ± 537.6[a]	20.4 ± 9.0	0.015 ± 0.006
500 ppm 2,6-DAT	5	2048.8 ± 860.8	17.8 ± 7.4	0.014 ± 0.004

[a]Total number of nuclei was significantly decreased compared to the basal diet treatment group.
*Significantly different from the basal diet group ($p < 0.01$).

These results suggest that both DATs are mutagenic in the presence of S9 activation *in vitro* and also that *O*-acetylation is important for the metabolic activation.

In Vivo Mutagenicity of 2,4-DAT

For the initial *in vivo* genotoxicity assay, we examined MN formation in the peripheral blood of F344 *gpt* delta rats treated with 2,4-DAT or 2,6-DAT. However, no significant increase in MN frequency was observed in any of the treated groups (Supplementary table 4).

Next, we examined the mutagenicity of the DATs in the livers and kidneys of the rats. *gpt* MFs were significantly increased in the livers of 2,4-DAT–treated rats at all three doses and in the DEN-positive control, compared to the control group (Fig. 3, Supplementary table 3). No increases in MFs were observed in the livers of 2,6-DAT–treated rats or in the kidneys of either 2,4-DAT– or 2,6-DAT–treated rats. To characterize the *gpt* mutations in the liver, we performed DNA sequencing (Table 3). The predominant base substitutions were G:C-to-A:T transitions and G:C-to-T:A and G:C-to-C:G transversions in the 2,4-DAT–treated groups. In addition, base substitutions at A:T bps were also induced. In the DEN-treated positive control group, A:T-to-T:A transversions were the most predominant type of mutation. Spi$^-$ MFs in the liver were also significantly increased in 2,4-DAT treatment groups at doses of 250 and 500 ppm and in the DEN-treated group (Table 4). They were not increased by treatment with 2,6-DAT. DNA sequence analysis revealed that the specific mutant frequency (SMF) of a −1 frameshift at run sequences such as GGGG in the *gam* gene was increased more than fourfold after treatment with 500 ppm 2,4-DAT, while the SMF of deletions of more than two bps was not enhanced at this dose (Supplementary table 5). Thus, most of the Spi$^-$ mutations were −1 frameshift mutations at run sequences, and large deletion mutations were not significantly induced by treatment with 2,4-DAT.

TABLE 2
Quantification of GST-P–Positive Foci

	No. of Rats	No. of Foci (No./cm^2)	Area of Foci (mm^2/cm^2)
Basal diet	5	0.00 ± 0.00	0.000 ± 0.000
Basal diet (DEN)	5	78.92 ± 17.70**	1.924 ± 0.655**
125 ppm 2,4-DAT	5	0.00 ± 0.00	0.000 ± 0.000
250 ppm 2,4-DAT	5	1.19 ± 1.21	0.022 ± 0.023
500 ppm 2,4-DAT	5	6.05 ± 3.93*	0.502 ± 0.476*
500 ppm 2,6-DAT	5	0.00 ± 0.00	0.000 ± 0.000

*Significantly different from the basal diet group ($p < 0.05$).
**Significantly different from the basal diet group ($p < 0.01$).

DISCUSSION

In the regulatory sciences, a default assumption is that genotoxic carcinogens have no thresholds for their activities, and thus, no acceptable daily intake can be set for these chemicals when they are used as food additives, pesticides, or veterinary medicines (Kirsch-Volders *et al.*, 2000; Nohmi, 2008). It is thought that single molecules of genotoxic compounds can induce mutations, and thus, genotoxic carcinogens impose carcinogenic risks to humans even at very low doses. However, how the genotoxicity of chemicals should be defined is not entirely clear. Currently, more than 200 genotoxicity assays have been proposed (Preston and Hoffmann, 2007). Unsurprisingly, the results among the various genotoxicity assays are inconsistent. The aromatic amine structural isomers 2,4-DAT and 2,6-DAT are an interesting reference pair that illustrates the inconsistency between *in vitro* and *in vivo* results (Cunningham *et al.*, 1989). Both 2,4-DAT and 2,6-DAT are mutagenic *in vitro* in *S. typhimurium* strains, but only 2,4-DAT is carcinogenic in mice and rats (NTP, 1979).

In this study, we confirmed *in vitro* genotoxicity with *S. typhimurium* TA98 and YG1024 and explored *in vivo* genotoxicity with F344 *gpt* delta rats. Both DATs were mutagenic in the *S. typhimurium* strains *in vitro* when the S9 activation system was present (Fig. 2). In contrast, only 2,4-DAT was mutagenic in the livers of rats (Fig. 3, Table 4, Supplementary table 4). Both *gpt* and Spi$^-$ MFs in the liver were significantly increased in 2,4-DAT–treated rats compared to those in the control group. We did not observe any increase in *gpt* MFs in the livers of 2,6-DAT–treated rats or in the kidneys of 2,4- or 2,6-DAT–treated rats (Fig. 3, Supplementary table 4). Kidney may not have capacity to activate 2,4-DAT as in the case of bone marrow (see below). We identified preneoplastic lesions (i.e., GST-P–positive foci) in the livers of rats treated with 250 and 500 ppm 2,4-DAT (Table 2) but not in the livers of rats treated with 2,6-DAT. Generally, proliferation is activated in cancer cells. Ki-67 is a nuclear marker of cell proliferation and detectable in cells at all phases of the cell cycles except G_0 (Gerdes *et al.*, 1983). The Ki-67

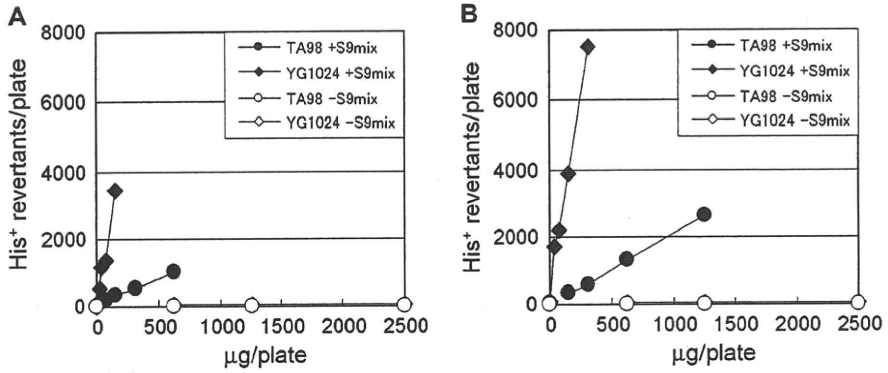

FIG. 2. Mutagenic activity of 2,4-DAT (A) and 2,6-DAT (B) in *Salmonella typhimurium* strains TA98 (circle) and YG1024 (rhombus). Filled circle and rhombus assayed with S9 mix; open circle and rhombus assayed without S9 mix.

labeling index is a measure of tumor proliferation and reported the association with liver and breast cancer outcome (de Azambuja *et al.*, 2007; Nolte *et al.*, 1998). The increase in Ki-67 index suggested the precancerous status of liver of rats treated by 2,4-DAT (Table 1, Fig. 1). We conclude from these results that genotoxicity assays (i.e., *gpt* and Spi$^-$ assays) and short-term carcinogenicity assays (i.e., GST-P–positive foci formation) can be conducted with F344 *gpt* delta rats. Because we observed genotoxicity in the target organ of carcinogenicity, these results strongly suggest that the carcinogenicity of 2,4-DAT is due to genotoxic activities. Integration of the genotoxicity assay with the pathological assay including GST-P–positive foci formation in *gpt* delta rats could reduce the number of animals necessary for these assays; this would contribute to the adoption of the 3R (reduction, replacement, and refinement) principle for animal use in the life sciences (Balls, 1997). It should be mentioned, however, that GST-P–positive foci formation often needs long treatment periods, for example, 16 and 24 weeks, respectively, for 2-amino-3,8-dimethylimidazo[4,5-*f*]-quinoxaline and 2-acetylaminofluorene (Bagnyukova *et al.*, 2008; Tsuda *et al.*, 2003) and such long treatments may increase the risk of false-positive results of mutations due to nongenotoxic mechanisms caused by chronic toxicity, for example, tumor induction and inflammatory responses (Thybaud et al., 2003).

Why do both 2,6-DAT and 2,4-DAT exhibit mutagenicity *in vitro*? The inconsistency between *in vitro* and *in vivo* results could be due to the different metabolic pathways of 2,6-DAT *in vitro* and *in vivo*. It is plausible that a DAT amino group is first oxidized by a specific cytochrome P450 (e.g., CYP1A2), and the resulting *N*-hydroxy group is further activated by OAT, which leads to the generation of nitrenium ions that can bind to DNA *in vitro* (Watanabe *et al.*, 1994). *In vitro,* both DATs were mutagenic only in the presence of S9 activation, and strain YG1024, which overexpresses OAT, exhibited greater sensitivity to the DATs than did strain TA98 (Fig. 2). Both *S. typhimurium* strains possess GC repetitive sequences in the *hisD* gene that serve as target sites for mutations. We speculate, therefore, that 2,4-DAT could be activated *in vivo* via the pathway described above and induce mostly guanine adducts in DNA. In fact, it was reported that 2,4-DAT induces DNA

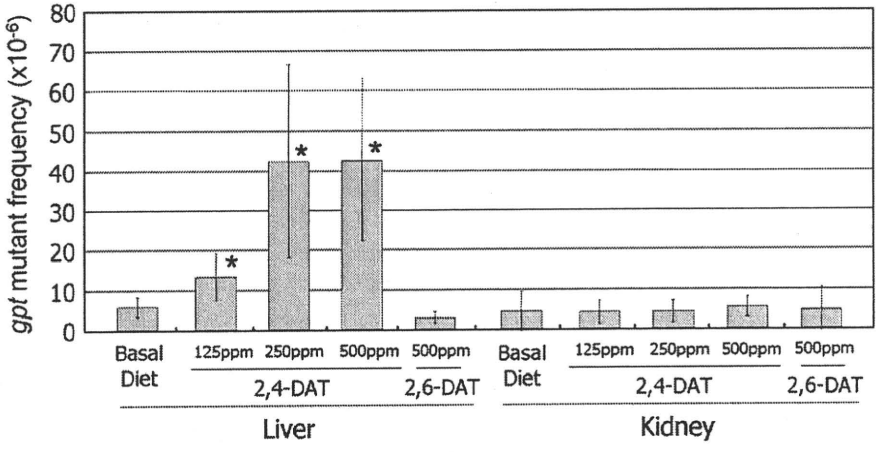

FIG. 3. MFs of *gpt* genes. Values represent mean SD ($n = 5$). Significant differences were observed in 2,4-DAT–treated livers compared to livers from rats fed negative control basal diet. *$p < 0.05$.

TABLE 3
Classification of *gpt* Mutations in *gpt* Delta Rat Livers

Type of gpt Mutation	Basal Diet		125 ppm 2,4-DAT		250 ppm 2,4-DAT		500 ppm 2,4-DAT		500 ppm 2,6-DAT		Basal Diet (DEN)	
	No.	%	No.	%	No.	%	No.	%	No.	%	No.	%
Base substitution												
Transition												
G:C → A:T	4	22	15	26	18	38	12	35	4	27	13	22
(CpG)	(1)		(6)		(6)		(3)		(1)		(3)	
A:T → G:C	1	6	1	2	5	11	1	3	3	20	12	21
Transversion												
G:C → T:A	4	22	16	28	12	26	6	18	4	27	3	5
G:C → C:G	1	6	7	12	4	9	7	21	0	0	0	0
A:T → T:A	0	0	5	9	4	9	1	3	1	7	23	40
A:T → C:G	1	6	4	7	3	6	1	3	0	0	7	12
Deletion												
−1	4	22	3	5	1	2	2	6	1	7	0	0
>2	2	11	2	3	0	0	1	3	2	13	0	0
Insertion	1	6	3	5	0	0	1	3	0	0	0	0
Others	0	0	2	3	0	0	2	6	0	0	0	0
Total	18	100	58	100	47	100	34	100	15	100	58	100

adducts in the livers of rats over 6000 times more efficiently than does 2,6-DAT (Taningher *et al.*, 1995). The sequence analysis that we conducted indicates that most of the mutations induced by 2,4-DAT at 500 ppm were guanine base substitutions; that is, G:C-to-A:T, G:C-to-T:A, and G:C-to-C:G (Table 3). 2,6-DAT might be more efficiently detoxicated than 2,4-DAT *in vivo* because its *para* site at position 4 can be oxidized and subsequently conjugated by phase II enzymes (Cunningham *et al.*, 1989). Detoxication of 2,6-DAT by phase II enzymes may be ineffective *in vitro* compared to *in vivo*. Appropriate cofactors, for example, uridine 5′-diphosphoric acid P2-β-D-glucopyranuronosyl ester for glucuronidation, may be needed to effectively detoxify the active metabolites of 2,6-DAT *in vitro*. At present, however, we cannot rule out the possibility that other factors, such as DNA repair, cell proliferation, translesion DNA synthesis, or apoptosis, might be involved in the differences in mutagenicity of 2,6-DAT *in vitro* and *in vivo*.

TABLE 4
Spi⁻ Mutant Frequency in Rat Livers

Treatment	No. of Rats	Mutant Frequency ($\times 10^{-6}$) (Mean ± SD)	*p* Value (*t*-test)
Basal diet	5	4.43 ± 1.99	
Basal diet (DEN)	5	341.22 ± 180.91	0.002
125 ppm 2,4-DAT	5	8.20 ± 4.75	0.07
250 ppm 2,4-DAT	5	13.42 ± 4.83	0.003
500 ppm 2,4-DAT	5	15.98 ± 4.45	0.0004
500 ppm 2,6-DAT	5	5.49 ± 2.53	0.241

In addition to the discrepancy between *in vitro* and *in vivo* mutagenicity, neither 2,4-DAT nor 2,6-DAT was genotoxic in the bone marrows of rats according to the MN assay (Supplementary table 3). 2,4-DAT is also not mutagenic when applied to MutaMouse skin (Kirkland and Beevers, 2006). Thus, we suggest that the negative results of the MN assay may be due to inefficient metabolic activation of 2,4-DAT at extrahepatic sites. Alternatively, the active metabolites generated in the liver may not reach the bone marrow. The poor metabolic activation in extrahepatic sites and/or short half-lives of the active metabolites may also account for the negative results of the MN assay with DEN in the bone marrow (Supplementary table 3). The MN assay is usually the first choice for *in vivo* genotoxicity assays in the development of pharmaceuticals; our results indicate that rather than relying on the MN assay in the bone marrow, genotoxicity should be evaluated in multiple organs, including the target organs of carcinogenicity.

The Spi⁻ assay is unique to *gpt* delta mice and rats and identifies deletion-type mutations (Nohmi *et al.*, 2000). Previous studies with *gpt* delta mice suggested that genotoxic compounds and physical factors (e.g., radiation) induce different types of deletion mutations *in vivo* (Nohmi and Masumura, 2005). For example, heavy-ion radiation, ultraviolet B radiation, and mitomycin C induce large deletions in the liver, epidermis, and bone marrow, respectively, at molecular sizes of >1 kbp (Horiguchi *et al.*, 2001; Masumura *et al.*, 2002; Takeiri *et al.*, 2003). In contrast, aromatic amines such as 2-amino-1-methyl-6-phenylimidazo[4,5-b]pyridine (PhIP) and aminophenylnorharman (APNH) induce −1 frameshift mutations in runs of guanine bases in the colon and liver, respectively (Masumura *et al.*, 2000, 2003). We characterized Spi⁻ mutants obtained from the livers of rats treated with 500-ppm 2,4-DAT and concluded that, like PhIP and APNH, 2,4-DAT induces mostly −1 frameshift mutations (Supplementary table 5). These results suggest that Spi⁻ assay, as well as the *gpt* assay, is useful for characterizing mutations, which may constitute the molecular basis of chemically induced carcinogenesis.

At the 2006 International Conference on Harmonization of Technical Requirements for Registration of Pharmaceuticals for Human Use meeting held in Yokohama, Japan, revisions of the guidelines for a basic test battery of *in vitro* and *in vivo* genotoxicity tests were discussed (Hayashi, 2008). The current guidelines recommend two *in vitro* assays (Ames test and either a mammalian chromosome aberration test or a mammalian gene mutation test) plus one *in vivo* assay (usually MN test). Because of the high rate of false positives with *in vitro* mammalian cell assays (Kirkland *et al.*, 2005), however, an alternative test battery was proposed at the meeting (Hayashi, 2008). The new battery is composed of one *in vitro* assay (Ames test) plus two *in vivo* assays (MN test plus a second *in vivo* test such as a transgenic assay or *in vivo* comet assay). It is possible to choose the classical battery of two *in vitro* assays plus one

in vivo assay instead of the alternative new battery. With the 3R principle in mind, integration of *in vivo* genotoxicity assays and a 28-day repeated dose toxicity assay was also discussed. *In vivo* mutagenicity assays and an *in vivo* MN assay can be integrated into a 28-day repeated dose toxicity study when transgenic rodents are used (Thybaud *et al.*, 2003). In this study, we found that an *in vivo* genotoxicity assay and a short-term bioassay for liver carcinogenesis using GST-P–positive foci as an end point of preneoplastic lesions can be conducted with F344 *gpt* delta rats. Integration of the two assays using transgenic rats may further facilitate adoption of the 3R principle in regulatory toxicology.

SUPPLEMENTARY DATA

Supplementary data are available online at http://toxsci.oxfordjournals.org/.

FUNDING

Ministry of Education, Culture, Sports, Science and Technology, Japan (18201010); the Ministry of Health, Labour and Welfare, Japan (MHLW; H21-Food-General-009); the Japan Health Science Foundation (KHB1007); MHLW (20 designated-8).

REFERENCES

Aoki, Y., Hashimoto, A. H., Amanuma, K., Matsumoto, M., Hiyoshi, K., Takano, H., Masumura, K., Itoh, K., Nohmi, T., and Yamamoto, M. (2007). Enhanced spontaneous and benzo(a)pyrene-induced mutations in the lung of *Nrf2*-deficient *gpt* delta mice. *Cancer Res.* **67,** 5643–5648.

Bagnyukova, T. V., Tryndyak, V. P., Montgomery, B., Churchwell, M. I., Karpf, A. R., James, S. R., Muskhelishveli, L., Beland, F. A., and Pogribny, I. P. (2008). Genetic and epigenetic changes in rat preneoplastic liver tissue induced by 2-acetylaminofluorene. *Carcinogenesis* **29,** 638–646.

Balls, M. (1997). The three Rs concept of alternatives to animal experimentation. In *Animal Alternatives* (L. F. M. van Zutphen and M. Balls, Eds.), pp. 27–41. Elsevier, Amsterdam.

Cunningham, M. L., Burka, L. T., and Matthews, H. B. (1989). Metabolism, disposition, and mutagenicity of 2,6-diaminotoluene, a mutagenic non-carcinogen. *Drug Metab. Dispos.* **17,** 612–617.

Cunningham, M. L., Hayward, J. J., Shane, B. S., and Tindall, K. R. (1996). Distinction of mutagenic carcinogens from a mutagenic noncarcinogen in the big blue transgenic mouse. *Environ. Health Perspect.* **104**(Suppl. 3), 683–686.

de Azambuja, E., Cardoso, F., de Castro, G., Jr, Colozza, M., Mano, M. S., Durbecq, V., Sotiriou, C., Larsimont, D., Piccart-Gebhart, M. J., and Paesmans, M. (2007). Ki-67 as prognostic marker in early breast caner: a meta-analysis of published studies involving 12,155 patients. *Br. J. Cancer.* **96,** 1504–1513.

Eastmond, D. A., Hartwig, A., Anderson, D., Anwar, W. A., Cimino, M. C., Dobrev, I., Douglas, G. R., Nohmi, T., Phillips, D. H., and Vickers, C. (2009). Mutagenicity testing for chemical risk assessment: update of the WHO/IPCS Harmonized Scheme. *Mutagenesis* **24,** 341–349.

Gerdes, J., Schwab, U., Lemke, H., and Stein, H. (1983). Production of a mouse monoclonal antibody reactive with a human nuclear antigen associated with cell proliferation. *Int. J. Cancer* **31,** 13–20.

Hashimoto, A. H., Amanuma, K., Masumura, K., Nohmi, T., and Aoki, Y. (2009). *In vivo* mutagenesis caused by diesel exhaust in the testis of *gpt* delta mouse. *Genes Environ.* **31,** 1–8.

Hayashi, H., Kondo, H., Masumura, K., Shindo, Y., and Nohmi, T. (2003). Novel transgenic rat for in vivo genotoxicity assays using 6-thioguanine and Spi⁻selection. *Environ. Mol. Mutagen.* **41,** 253–259.

Hayashi, M. (2008). Update on the maintenance of the ICH S2 genetic toxicology. *Pharm. Regul. Sci.* **39,** 515–521.

Heddle, J. A., Dean, S., Nohmi, T., Boerrigter, M., Casciano, D., Douglas, G. R., Glickman, B. W., Gorelick, N. J., Mirsalis, J. C., Martus, H. J., *et al.* (2000). *In vivo* transgenic mutation assays. *Environ. Mol. Mutagen.* **35,** 253–259.

Horiguchi, M., Masumura, K. I., Ikehata, H., Ono, T., Kanke, Y., and Nohmi, T. (2001). Molecular nature of ultraviolet B light-induced deletions in the murine epidermis. *Cancer Res.* **61,** 3913–3918.

Ito, N., Imaida, K., Asamoto, M., and Shirai, T. (2000). Early detection of carcinogenic substances and modifiers in rats. *Mutat. Res.* **462,** 209–217.

Kirkland, D., Aardema, M., Henderson, L., and Muller, L. (2005). Evaluation of the ability of a battery of three *in vitro* genotoxicity tests to discriminate rodent carcinogens and non-carcinogens I. Sensitivity, specificity and relative predictivity. *Mutat. Res.* **584,** 1–256.

Kirkland, D., and Beevers, C. (2006). Induction of *LacZ* mutations in Muta Mouse can distinguish carcinogenic from non-carcinogenic analogues of diaminotoluenes and nitronaphthalenes. *Mutat. Res.* **608,** 88–96.

Kirsch-Volders, M., Aardema, M., and Elhajouji, A. (2000). Concepts of threshold in mutagenesis and carcinogenesis. *Mutat. Res.* **464,** 3–11.

Maron, D. M., and Ames, B. N. (1983). Revised methods for the salmonella mutagenicity test. *Mutat. Res.* **113,** 173–215.

Masumura, K., Matsui, M., Katoh, M., Horiya, N., Ueda, O., Tanabe, H., Yamada, M., Suzuki, H., Sofuni, T., and Nohmi, T. (1999). Spectra of *gpt* mutations in ethylnitrosourea-treated and untreated transgenic mice. *Environ. Mol. Mutagen.* **34,** 1–8.

Masumura, K., Matsui, K., Yamada, M., Horiguchi, M., Ishida, K., Watanabe, M., Wakabayashi, K., and Nohmi, T. (2000). Characterization of mutations induced by 2-amino-1-methyl-6-phenylimidazo[4,5-*b*]pyridine in the colon of *gpt* delta transgenic mouse: novel G: C deletions beside runs of identical bases. *Carcinogenesis* **21,** 2049–2056.

Masumura, K., Kuniya, K., Kurobe, T., Fukuoka, M., Yatagai, F., and Nohmi, T. (2002). Heavy-ion-induced mutations in the *gpt* delta transgenic mouse: comparison of mutation spectra induced by heavy-ion, X-ray, and gamma-ray radiation. *Environ. Mol. Mutagen.* **40,** 207–215.

Masumura, K., Totsuka, Y., Wakabayashi, K., and Nohmi, T. (2003). Potent genotoxicity of aminophenylnorharman, formed from non-mutagenic norharman and aniline, in the liver of *gpt* delta transgenic mouse. *Carcinogenesis* **24,** 1985–1993.

National Toxicology Program. (1979). Bioassay of 2,4-diaminotoluene for possible carcinogenicity. *Natl. Cancer Inst. Carcinog. Tech. Rep. Ser.* **162,** 1–139.

National Toxicology Program. (1980). Bioassay of 2,6-toluenediamine dihydrochloride for possible carcinogenicity (CAS No. 15481-70-6). *Natl. Toxicol. Program Tech. Rep. Ser.* **200,** 1–123.

Nohmi, T. (2008). Possible mechanisms of practical thresholds for genotoxicity. *Genes Environ.* **30,** 108–113.

Nohmi, T., Katoh, M., Suzuki, H., Matsui, M., Yamada, M., Watanabe, M., Suzuki, M., Horiya, N., Ueda, O., Shibuya, T., *et al.* (1996). A new

transgenic mouse mutagenesis test system using Spi⁻and 6-thioguanine selections. *Environ. Mol. Mutagen.* **28,** 465–470.

Nohmi, T., and Masumura, K. (2005). Molecular nature of intrachromosomal deletions and base substitutions induced by environmental mutagens. *Environ. Mol. Mutagen.* **45,** 150–161.

Nohmi, T., Suzuki, T., and Masumura, K. (2000). Recent advances in the protocols of transgenic mouse mutation assays. *Mutat. Res.* **455,** 191–215.

Nolte, M., Werner, M., Nasarek, A., Bektas, H., von Wasielewski, R., Klempnauer, J., and Georgii, A. (1998). Expression of proliferation associated antigens and detection of numerical chromosome aberrations in primary human liver tumors: relevance to tumor characteristic and prognosis. *J. Clin. Pathol.* **51,** 47–51.

Ogiso, T., Tatematsu, M., Tamano, S., Tsuda, H., and Ito, N. (1985). Comparative effects of carcinogens on the induction of placental glutathione S-transferase-positive liver nodules in a short-term assay and of hepatocellular carcinomas in a long-term assay. *Toxicol. Pathol.* **13,** 257–265.

Preston, R. J., and Hoffmann, G. R. (2007). Genetic toxicology. In *Casarett and Doull's Toxicology: The Basic Science of Poisons* (C. D. Klaassen, Ed.), pp. 381–413. The McGraw-Hill Companies, Inc., New York.

Shibata, A., Maeda, D., Ogino, H., Tsutsumi, M., Nohmi, T., Nakagama, H., Sugimura, T., Teraoka, H., and Masutani, M. (2009). Role of Parp-1 in suppressing spontaneous deletion mutation in the liver and brain of mice at adolescence and advanced age. *Mutat. Res.* **664,** 20–27.

Takeiri, A., Mishima, M., Tanaka, K., Shioda, A., Ueda, O., Suzuki, H., Inoue, M., Masumura, K., and Nohmi, T. (2003). Molecular characterization of mitomycin C-induced large deletions and tandem-base substitutions in the bone marrow of *gpt* delta transgenic mice. *Chem. Res. Toxicol.* **16,** 171–179.

Taningher, M., Peluso, M., Parodi, S., Ledda-Columbano, G. M., and Columbano, A. (1995). Genotoxic and non-genotoxic activities of 2,4- and 2,6-diaminotoluene, as evaluated in Fischer-344 rat liver. *Toxicology* **99,** 1–10.

Thybaud, V., Dean, S., Nohmi, T., de Boer, J., Douglas, G. R., Glickman, B. W., Gorelick, N. J., Heddle, J. A., Heflich, R. H., Lambert, I., *et al.* (2003). *In vivo* transgenic mutation assays. *Mutat. Res.* **540,** 141–151.

Tsuda, H., Fukushima, S., Wanibuchi, H., Morimura, K., Nakae, D., Imaida, K., Tatematsu, M., Hirose, M., Wakabayashi, K., and Moore, M. A. (2003). Value of GST-P positive preneoplastic hepatic foci in dose-response studies of hepatocarcinogenesis: evidence for practical thresholds with both genotoxic and nongenotoxic carcinogens. A review of recent work. *Toxicol. Pathol.* **31,** 80–86.

Umemura, T., Kanki, K., Kuroiwa, Y., Ishii, Y., Okano, K., Nohmi, T., Nishikawa, A., and Hirose, M. (2006). *In vivo* mutagenicity and initiation following oxidative DNA lesion in the kidneys of rats given potassium bromate. *Cancer Sci.* **97,** 829–835.

Umemura, T., Tasaki, M., Kijima, A., Okamura, T., Inoue, T., Ishii, Y., Suzuki, Y., Masui, N., Nohmi, T., and Nishikawa, A. (2009). Possible participation of oxidative stress in causation of cell proliferation and *in vivo* mutagenicity in kidneys of *gpt* delta rats treated with potassium bromate. *Toxicology* **257,** 46–52.

Watanabe, M., Igarashi, T., Kaminuma, T., Sofuni, T., and Nohmi, T. (1994). N-hydroxyarylamine *O*-acetyltransferase of Salmonella typhimurium: proposal for a common catalytic mechanism of arylamine acetyltransferase enzymes. *Environ. Health Perspect.* **102**(Suppl. 6), 83–89.

Xu, A., Smilenov, L. B., He, P., Masumura, K., Nohmi, T., Yu, Z., and Hei, T. K. (2007). New insight into intrachromosomal deletions induced by chrysotile in the *gpt* delta transgenic mutation assay. *Environ. Health Perspect.* **115,** 87–92.

Published online 25 November 2009

Nucleic Acids Research, 2010, Vol. 38, No. 3 ***859–867***
doi:10.1093/nar/gkp1095

Critical amino acids in human DNA polymerases η and κ involved in erroneous incorporation of oxidized nucleotides

Atsushi Katafuchi[1], Akira Sassa[1,2], Naoko Niimi[1], Petr Grúz[1], Hirofumi Fujimoto[3], Chikahide Masutani[4], Fumio Hanaoka[5], Toshihiro Ohta[2] and Takehiko Nohmi[1,*]

[1]Division of Genetics and Mutagenesis, National Institute of Health Sciences, 1-18-1 Kamiyoga, Setagaya-ku, Tokyo 158-8501, [2]School of Life Sciences, Tokyo University of Pharmacy and Life Sciences, Hachiouji-shi, Tokyo 192-0392, [3]Division of Radiological Protection and Biology, National Institute of Infectious Diseases, 1-23-1 Toyama, Shinjuku-ku, Tokyo 162-8640, [4]Graduate School of Frontier Biosciences, Osaka University and SORST, JST, 1-3 Yamada-oka, Suita, Osaka 565-0871 and [5]Faculty of Science, Gakushuin University, 1-5-1 Mejiro, Toshima-ku, Tokyo 171-8588, Japan

Received September 22, 2009; Revised and Accepted November 6, 2009

ABSTRACT

Oxidized DNA precursors can cause mutagenesis and carcinogenesis when they are incorporated into the genome. Some human Y-family DNA polymerases (Pols) can effectively incorporate 8-oxo-dGTP, an oxidized form of dGTP, into a position opposite a template dA. This inappropriate G:A pairing may lead to transversions of A to C. To gain insight into the mechanisms underlying erroneous nucleotide incorporation, we changed amino acids in human Polη and Polκ proteins that might modulate their specificity for incorporating 8-oxo-dGTP into DNA. We found that Arg61 in Polη was crucial for erroneous nucleotide incorporation. When Arg61 was substituted with lysine (R61K), the ratio of pairing of dA to 8-oxo-dGTP compared to pairing of dC was reduced from 660:1 (wild-type Polη) to 7:1 (R61K). Similarly, Tyr112 in Polκ was crucial for erroneous nucleotide incorporation. When Tyr112 was substituted with alanine (Y112A), the ratio of pairing was reduced from 11:1 (wild-type Polκ) to almost 1:1 (Y112A). Interestingly, substitution at the corresponding position in Polη, i.e. Phe18 to alanine, did not alter the specificity. These results suggested that amino acids at distinct positions in the active sites of Polη and Polκ might enhance 8-oxo-dGTP to favor the *syn* conformation, and thus direct its misincorporation into DNA.

INTRODUCTION

Reactive oxygen species (ROS) are constantly generated in cells during normal aerobic metabolism. The intracellular levels of ROS are further enhanced by exposure of cells to redox agents or ionizing radiation (1–3). To counteract the potential genotoxicity and cytotoxicity of ROS, cells possess a number of defense systems, e.g. low-molecular-weight scavengers, ROS-degrading enzymes and DNA repair. Nevertheless, some ROS molecules escape the defense systems and eventually damage nearby bio-molecules including DNA, proteins and membrane lipids. Therefore, ROS has been implicated in the etiology of human degenerative diseases, aging and cancer (4,5).

DNA precursors (dNTPs) in the cellular nucleotide pool are subject to oxidation by ROS (6,7). Oxidized forms of DNA precursors include 7,8-dihydro-8-oxo-dGTP (8-oxo-dGTP), 7,8-dihydro-8-oxo-dATP (8-oxo-dATP) and 1,2-dihydro-2-oxo-dATP (2-OH-dATP). These oxidized dNTPs cause various deleterious effects in cells. For example, 8-oxo-dGTP can be incorporated opposite a dA residue in the template strand during DNA replication; this can result in an A to C transversion (8). *Escherichia coli* mutants deficient in the *mutT* gene, whose gene product hydrolyzes 8-oxo-dGTP, display spontaneous A to C transversion rates that are over 1000 times higher than those in wild-type strains (9,10). Similarly, 2-OH-dATP can be incorporated opposite template dG, and this induces G to T transversions. *Escherichia coli* mutants deficient in the *orf135* gene, whose gene product hydrolyzes 2-OH-dATP, display higher spontaneous G to T transversion rates than the

*To whom correspondence should be addressed. Tel: +81 3 3700 9872; Fax: +81 3 3700 2348; Email: nohmi@nihs.go.jp

wild-type strains (11,12). In higher-order organisms, the human MTH1 gene product, a functional counterpart of the *E. coli* MutT protein, hydrolyzes 8-oxo-dGTP, 8-oxo-dATP and also 2-OH-dATP; in contrast, MutT does not hydrolyze 2-OH-dATP (13,14). Overexpression of hMTH1 reduced total cellular 8-oxo-dG levels in human cells and transgenic mice. This overexpression also suppressed genome instability in cells with defective mismatch repair mechanisms; in addition, it caused delayed cellular senescence, and ameliorated neuropathological and behavioral symptoms in mice that resembled those of Huntington's disease (15,16). Alternatively, suppression of hMTH1 expression induced genomic DNA damage and caused accelerated cellular senescence in human skin fibroblasts (17). Mice deficient in the *Mth1* gene exhibited increased tumorigenicity in the lung, liver and stomach compared to wild-type mice (18). Thus, the nucleotide pool is a critical target of intracellular ROS, and oxidized nucleotides, unless continuously eliminated, can induce a variety of cellular abnormalities.

To exert these adverse effects, oxidized dNTPs must be incorporated into the genome DNA. Actually, in culture medium, 8-oxo-dG is readily incorporated into the genome DNA upon phosphorylation in human cells (19). Interestingly, Y-family DNA polymerases (Pols), a novel family of Pols involved in translesion DNA synthesis (20), efficiently and almost exclusively incorporated 8-oxo-dGTP into the DNA chain opposite a template dA (21). This specificity for erroneous pairing appears to be conserved in all Y-family Pols from bacteria, Archea and humans that have been examined. In *E. coli*, two Y-family Pols, i.e. Pol IV (DinB) and Pol V (UmuD′C), were involved in the erroneous incorporation of 8-oxo-dGTP and 2-OH-dATP into DNA in the *sod fur* mutants. In these mutants, intracellular ROS levels were elevated and, hence, the rates of spontaneous A to C and G to T transversions were elevated (22). The human Y-family Polη efficiently paired 8-oxo-dGTP with template dA (23). The incorporation of 8-oxo-dGTP into the genome of phage M13 by human Polη *in vitro* induced A to C transversions and deletions (24). In human cells, 8-oxo-dGTP induced an increase in the frequency of A to C mutations in the *supF* gene; this mutation frequency was reduced with the suppression of REV1, Polη and Polζ expression (25).

It has been shown that 8-oxo-dG assumes the *anti* conformation when it pairs with dC, but it assumes the *syn* conformation when pairing with dA (26,27). Therefore, we hypothesized that certain amino acids in the active sites of the Y-family Pols might force 8-oxo-dGTP to assume the *syn* conformation. In this study, we tested this hypothesis by amino acid substitutions of two Y-family human polymerases, Polη and Polκ. We changed three amino acids that might affect the specificity for pairing 8-oxo-dGTP with a template dA (28). The first candidates for amino acid alterations were the 'steric gate' amino acids, i.e. phenylalanine 18 (F18) of Polη and tyrosine 112 (Y112) in Polκ. These amino acids distinguish dNTPs and rNTPs by sensing their 2′-OH-groups (29). We reasoned that the proximity of these amino acids to the incoming dNTPs might play a critical role in determining the conformation of 8-oxo-dGTP. The second candidate for an amino acid alteration was arginine 61 (R61) in human Polη. This is the counterpart of yeast R73, which is located adjacent to the base of the incoming dNTP and stabilize dNTPs during bypass DNA synthesis across cisplatin adducts and cyclobutane pyrimidine dimers (30). The arginine residue is conserved in yeast and humans, but not in other Y-family Pols, including Polκ. The third candidate for an amino acid alteration was isoleucine 48 (I48) in Polη, which is the counterpart of yeast I59. This residue is also located close to the base of the dNTPs in the active site (30). Our results suggested that R61 in Polη and Y112 in Polκ were critical for the preferential pairing of 8-oxo-dGTP with template dA. This implies that distinctly positioned amino acids in the active sites of two Y-family Pols direct the conformation of the incoming 8-oxo-dGTP to the *syn* conformation. We discuss how R61 modulates the conformation of the incoming 8-oxo-dGTP in the active site of Polη.

MATERIALS AND METHODS

Substrates and enzymes

All oligonucleotides were purchased from BEX Corp. (Tokyo). Unaltered dNTPs were purchased from GE-Healthcare and oxidized dNTPs, i.e. 8-oxo-dGTP and 8-oxo-dATP, were purchased from TriLink BioTechnologies. 2-OH-dATP was kindly provided by Dr H. Kamiya (Hokkaido University). Human Polκ and the mutant Polκ with an alanine substitution at Y112 (Y112A) were prepared as described previously (31). The human Polη mutant enzymes included substitutions at F18 with alanine (F18A), at R61 with alanine, methionine, asparagine, glutamine, histidine or lysine (R61A, R61M, R61N, R61Q, R61H or R61K), and at I48 with serine, methionine, phenylalanine, asparagine or glutamine (I48S, I48M, I48F, I48N or I48Q). Polη and its mutant proteins were prepared with the pET21bXPV(1-511) plasmid that carried the human Polη cDNA sequence. Site-directed mutagenesis protocols were used to exchange the DNA sequences that encoded the targeted amino acids (QuickChange Lightening Site-Directed Mutagenesis Kit; STRATAGENE). The resulting plasmids were transformed into Rosetta (DE3) plysS cells (Novagen). The cells were grown in 1 l of Luria–Bertani (LB) medium until the cell density reached an OD_{600} = 0.6. The expression of Polη and the mutant proteins were induced with the addition of 0.2 mM IPTG at 15°C for 10 h (32). The resulting cell pastes were resuspended in lysis buffer comprised of 50 mM potassium phosphate buffer pH 7.0, 500 mM NaCl, 10% sucrose, 20% glycerol, 1× BugBuster (Novagen), 5 mM imidazole, 5 mM β-mercaptoethanol, benzonase nuclease (Novagen) and complete EDTA-free, which is a protease inhibitor cocktail (Roche). The resuspended mixtures were incubated on ice for 30 min. The lysates were clarified by centrifugation at 20 000*g* for 20 min at 4°C. TALON super flow metal affinity resin (Clontech) was washed twice with

wash buffer (50 mM potassium phosphate buffer pH 7.0, 500 mM NaCl, 10% glycerol, 10 mM imidazole, 5 mM β-mercaptoethanol, complete EDTA-free), and the washed resin was gently mixed with the supernatant containing the Polη or the mutant proteins for 30 min. After three subsequent washings, the resins were placed on the column, and washed twice. The Polη and the mutant proteins were eluted with 5 ml of elution buffer (the wash buffer plus 350 mM imidazole). For kinetics analyses, the proteins were further purified with HiLoad 16/60 Superdex 200 pg and HiTrap Heparin HP columns (both from GE Healthcare) with an FPLC system (AKTAexplorer 10 s, GE Healthcare). The pooled fractions containing wild-type hPolη, R61A and R61K were dialyzed against 25 mM Tris–HCl pH 7.5, 2.5 mM β-mercaptoethanol and 50% glycerol. All purified proteins were stored at −80°C.

Incorporation of oxidized dNTPs

DNA extension assays were performed to test the behavior of the native and mutant Pols. The DNA primers used in the DNA extension assays were annealed with the template DNA sequence (5′-GAAGG GATCCTTAAGACNGTAACCGGTCTTCGCGCG-3′, where N represents A, C, G or T) at a molar ratio of 1 : 1.2. The template/primer (100 nM) was combined with appropriate concentrations of Polη (5 nM), Polκ (10 nM) and mutant proteins (5, 50 or 100 nM), and incubated in a reaction buffer [40 mM Tris–HCl (pH 8.0), 5 mM $MgCl_2$, 10 mM dithiothreitol, 100 μg/ml BSA, 60 mM KCl, 2.5% glycerol] with 50 μM of oxidized dNTPs for 10 min at 37°C. The exact concentrations of proteins are described in legends of figures and Supplementary Figures. Reactions were terminated by addition of the termination buffer (98% formamide, 10 mM EDTA, 10 mg/ml Blue dextran). After heat denaturation, the mixtures were loaded onto a denaturing 15% polyacrylamide gel for electrophoresis (PAGE), and run with a buffer containing 8 M urea. The products were visualized with a Molecular Imager FX Pro System (Bio-Rad Laboratories) and quantified with Quantity One software (Bio-Rad Laboratories). For steady-state kinetic analyses of incorporation of oxidized dNTP, the reactions were carried out with 1 nM Polη and 5 nM Polκ. Both the concentrations of dNTP and the incubation times were varied according to the activity of a given enzyme. The products were analyzed as described in the primer extension assay. The rate of incorporation was plotted against dNTP concentrations, and the apparent Michaelis–Menten constant, K_m and V_{max} values were determined by Enzyme Kinetics Module 1.1 of SigmaPlot 2001 software (SPSS Inc., IL). The k_{cat} was calculated by dividing the V_{max} by the enzyme concentration. All values represent means plus standard errors from three independent experiments.

Translesion DNA synthesis assay

Primer DNA (5′-CTTCCCTAGGAATTCTGC-3′) labeled with Cy3 at the 5′-end was annealed to template DNA (5′-GCGCGCTTCTGGCCAATXGCAGAATTC CTAGGGAAG-3′, where X represents 8-oxo-dG or 8-oxo-dA) at a molar ratio of 1:1.2. Similarly, primer DNA (5′-CTTCCCTAGGAATT-3′) labeled with Cy3 at the 5′-end was annealed with template DNA (5′-GCGCG CTTCTGGCCAATTGCAGAATTCCTAGGGAAG-3′, where TT represents a *cis-syn* thymine dimer) at a ratio of 1 : 1.2. The template/primer containing 8-oxo-dG or 8-oxo-dA were incubated with 5 nM of Polη and R61K, or 10 nM of wild-type Polκ and 100 nM of Y112A. The reaction buffer contained 5 μM of unaltered dNTPs, and the reactions were incubated for 10 min at 37°C. The template/primer that contained the thymine dimer was incubated with 1, 5 and 20 nM of either wild-type Polη or R61K in the reaction buffer. This reaction buffer contained 250 μM dNTPs, and the reactions were incubated for 5 min at 37°C. The products were analyzed as described earlier.

Modeling 8-oxo-dGTP in the active site of Polη

Models were created of 8-oxo-dGTP in the *syn* conformation opposite a dA residue and in the *anti* conformation opposite a dC residue in the active site of yeast Polη by 2007.09 version of the Molecular Operating Environment (MOE: Chemical Computing Group Inc., Montreal, Canada). These models were based on the reported crystallographic structures [PDB#: 2R8J (21)]. The active site of yeast Polη was displayed with Gaussian surfaces. The template and primer sequences were 3′-CACCTACT CX-5′ and 5′-GTGGATGAG-3′, respectively, where X represents the dA or dC that was paired with 8-oxo-dGTP.

RESULTS

The steric gate of Polκ is involved in the orientation of incoming 8-oxo-dGTP

The steric gate amino acids, which distinguish between dNTP and rNTP, are highly conserved. In most Pols, including those in the Y-family, phenylalanine or tyrosine forms the steric gate (29). In human Polκ, Y112 acts as the steric gate and also plays important roles in both the insertion of dCTP opposite a benzo[a]pyrene diolepoxide-N^2-dG adduct in the template DNA and the extension of mismatched termini (31). In Polη, F18 is assumed to be the steric gate, based on the amino acid sequence alignment and the crystallographic structure comparison with yeast Polη (Supplementary Figure S1) (30,33,34). We found that the mutant of Polη with the alanine substitution of F18 (F18A) was able to incorporate both rNTPs and dNTPs into DNA. However, its ability to incorporate dNTPs was substantially attenuated compared to the native Pol (data not shown). As the steric gates lie adjacent to the incoming dNTPs, they may affect the specificity incorporating oxidized dNTPs into DNA. To examine the possibility, we compared the specificities of Polκ versus Y112A and Polη versus F18A for preferentially pairing 8-oxo-dGTP with template dA. We found that Polκ showed a preference for pairing 8-oxo-dGTP with template dA (Figure 1A). However, this preferential pairing was absent in Y112A, which

paired 8-oxo-dGTP with both dA and dC with nearly equal frequency. The kinetic analyses indicated that the substitution of Y112 with alanine reduced the efficiency (k_{cat}/K_m) of pairing 8-oxo-dGTP with template dA by more than 200-fold. This resulted in nearly equal frequencies of pairing 8-oxo-dGTP with template dA and dC (Table 1). In contrast, both the wild-type Polκ and the Y112A mutant showed similar specificities for mainly incorporating 8-oxo-dATP opposite dT and 2-OH-dATP with dT and dG (Figure 1B and C).

We also examined the specificity of wild-type Polκ and Y112A for translesion DNA synthesis across 8-oxo-dG and 8-oxo-dA lesions in template strands. We found that both Pols had similar specificity for inserting dATP and, less frequently dCTP, opposite a template 8-oxo-dG; both also preferentially inserted dTTP opposite to a template 8-oxo-dA (Supplementary Figure S2). These

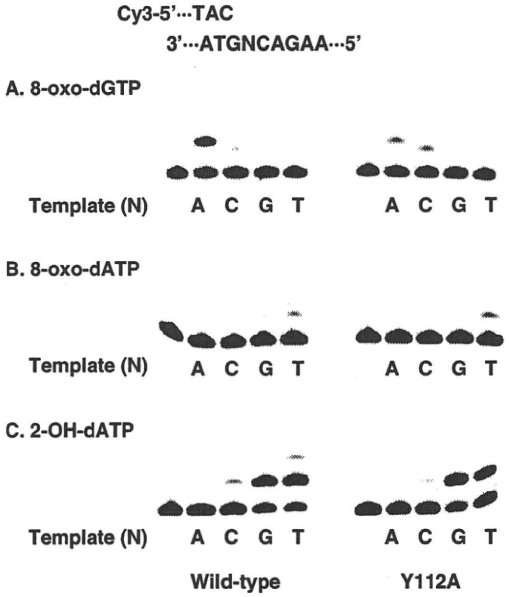

Figure 1. Incorporation of oxidized dNTPs into DNA by Polκ and its Y112A mutant. The primer/template DNA (100 nM, N in the template strand represents A, C, G or T) was incubated with wild-type Polκ (10 nM) or Y112A mutant (100 nM) in the presence of 50 μM 8-oxo-dGTP (**A**), 8-oxo-dATP (**B**) or 2-OH-dATP (**C**) for 10 min at 37°C. Extended primers were separated by denaturing PAGE. The first lanes represent the results of control experiments where no dNTPs were added to the reaction mixtures.

data indicated that the Y112 residue in Polκ was involved in the orientation of incoming 8-oxo-dGTP opposite dA, but not other specificity, i.e. incorporating 8-oxo-dATP or 2-OH-dATP into DNA or for a translesion bypass across an oxidized dG or dA in template strands.

In Polη, the corresponding substitution of F18 by alanine did not alter the specificity for incorporating oxidized dNTPs, including 8-oxo-dGTP, into DNA (Supplementary Figure S3). Therefore, we concluded that the steric gate of Polκ, but not Polη, was critical for inducing incoming 8-oxo-dGTP into the *syn* conformation in the active site, thereby facilitating its pairing with dA.

R61 of Polη determines specificity for pairing 8-oxo-dGTP with template dA

As F18 did not appear to be involved in the orientation of 8-oxo-dGTP in the active site of Polη, we investigated other amino acids that might influence its specificity for incorporating 8-oxo-dGTP into DNA. We reasoned that R61 was the best candidate, because it was predicted to lie adjacent to the base of the incoming dNTP. Thus, we substituted R61 with alanine, methionine, asparagine, glutamine, histidine or lysine. We also changed I48 to alanine, serine, methionine, phenylalanine, asparagine, glutamine, aspartic acid or glutamic acid because it was also predicted to lie close to the base of the incoming dNTP. We found that R61A, R61M, R61N, R61Q, R61H and all the I48 mutants displayed similar specificity to the wild-type Polη and/or exhibited extremely low abilities to incorporate 8-oxo-dGTP into DNA (Supplementary Figure S4). However, we found that R61K was able to pair 8-oxo-dGTP with dC or dA with nearly equal specificity (Figure 2A). In contrast, the wild-type Polη preferentially paired 8-oxo-dGTP with dA (Figure 2A). In addition to changing the preference for incorrect pairing of 8-oxo-dGTP, R61K paired 8-oxo-dATP more efficiently with dT than with dG. In contrast, the wild-type Polη showed almost equal specificity for pairing 8-oxo-dATP with dT and dG (Figure 2B). However, R61K exhibited equal specificity for pairing 2-OH-dATP with dG, dT and dC, and less efficiency for pairing with dA; this specificity was similar to that observed for the wild-type Polη (Figure 2C). The wild-type Polη and R61K showed similar translesion activities for DNA synthesis across 8-oxo-dG, 8-oxo-dA, or a thymine dimer in the template strands

Table 1. Steady-state kinetic parameters for 8-oxo-dGTP by wild-type Polκ and Y112A mutant

Template/dNTP	k_{cat}, min^{-1}		K_m, μM		k_{cat}/K_m, μM^{-1} min^{-1}		Y112A/WT
	WT[a]	Y112A	WT	Y112A	WT	Y112A	
dA/dTTP	14 ± 3.0	9.2 ± 3.5	4.3 ± 2.0	72 ± 52	3.3	0.13	1/26
dA/8-oxo-dGTP	2.1 ± 0.38	0.029 ± 0.0052	83 ± 34	300 ± 140	0.026	0.000096	1/270
dC/dGTP	4.4 ± 0.64	5.4 ± 0.33	2.1 ± 0.84	20 ± 3.4	2.1	0.28	1/7.7
dC/8-oxo-dGTP	0.70 ± 0.12	0.11 ± 0.030	290 ± 120	660 ± 360	0.0024	0.00016	1/15

[a]WT: wild-type Polκ

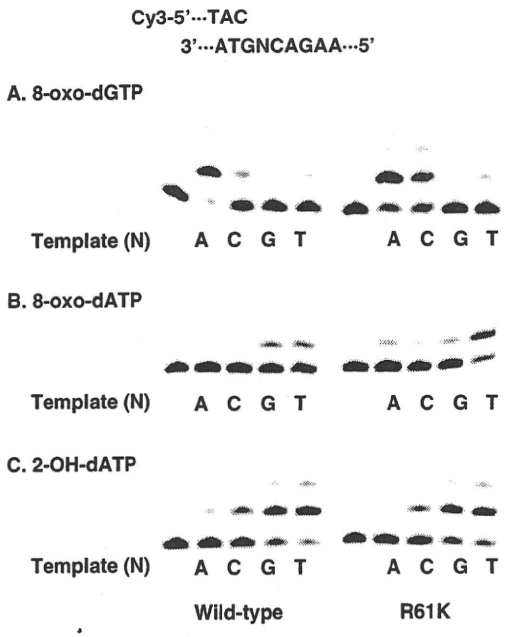

Figure 2. Incorporation of oxidized dNTPs into DNA by Polη and its R61K mutant. The primer/template DNA (100 nM, N in the template strand represents A, C, G or T) was incubated with wild-type Polη and R61K mutant (5 nM) in the presence of 50 μM 8-oxo-dGTP (**A**), 8-oxo-dATP (**B**) or 2-OH-dATP (**C**) for 10 min at 37°C. Extended primers were separated by denaturing PAGE. The first lanes represent the results of control experiments where no dNTPs were added to the reaction mixtures.

(Supplementary Figure S5). Thus, the effect of the R61K mutation appeared to be specific for conferring specificity for the incorporation of 8-oxo-dGTP and 8-oxo-dATP into DNA.

To quantitatively compare the efficiencies (k_{cat}/K_m) of incorporating 8-oxo-dGTP and 8-oxo-dATP into DNA among the wild-type Polη, R61K and R61A, we determined the kinetic parameters of each Pol for incorporating unaltered and oxidized dNTPs into DNA (Table 2). We found that the kinetic parameters for pairing unaltered dNTPs with the correct template bases were almost identical between the wild-type Polη and R61K. Likewise, the kinetics were not substantially different between the two Pols for pairing 8-oxo-dGTP and 8-oxo-dATP with incorrect template bases (8-oxo-dGTP with dA and 8-oxo-dATP with dG). However, R61K exhibited efficiencies that were 24-fold and 14-fold higher than wild type for correctly pairing 8-oxo-dGTP with dC and pairing 8-oxo-dATP with dT. Similarly, R61A exhibited efficiencies that were 1.7-fold higher than wild type for pairing both 8-oxo-dGTP and 8-oxo-dATP with dC and dT, respectively. These results suggested that R61 in Polη specifically inhibited pairing the C8-oxidized deoxypurine triphosphates with the correct template bases; i.e. 8-oxo-dGTP with dC and 8-oxo-dATP with dT. We concluded, therefore, that R61 was critical for orienting the incoming 8-oxo-dGTP into the *syn* conformation in the active site of Polη.

DISCUSSION

Oxidation of the nucleotide pool can be a source of DNA damage when oxidized dNTPs are incorporated into DNA by Pols during chromosome replication (35). However, oxidized dNTPs are generally poor substrates for Pols. For example, calf thymus Polδ incorporated 8-oxo-dGTP into DNA with only about 10^{-4} times the efficiency showed for incorporating unaltered dGTP; moreover, the Pol exhibited a preference for correctly pairing 8-oxo-dGTP with template dC (36). Several other Pols exhibited poor efficiencies for 8-oxo-dGTP incorporation into DNA, including human Polγ, T7 Pol exo$^-$, HIV reverse transcriptase, *E. coli* Pol II, ϕ29 Pol and Klenow exo$^-$ (37,38). An exception may be human Polβ, which incorporated 8-oxo-dGTP into DNA with 10–20% of the efficiency it showed for unaltered dGTP incorporation, and it showed a preference for incorrect pairing with template dA (39). Calf thymus Polα incorporated 2-OH-dATP with <1% and 0.1% of the efficiencies it showed for incorporating unaltered dATP and dGTP, respectively; moreover, the Pol showed a similar preference for pairing 2-OH-dATP with template T and C (40). In this respect, it is interesting that Y-family Pols from bacteria, Archaea and humans exhibit a preference for incorrectly pairing 8-oxo-dGTP with template dA (21,22,24) and human Polη incorporates it with a relatively high efficiency (23,41).

To examine the mechanisms underlying the conserved specificity of Y-family Pols for incorrectly pairing 8-oxo-dGTP with template dA, we substituted amino acids of human Polη and Polκ, which might modulate the specificity. The results indicated that R61 of Polη and Y112 of Polκ played important roles in the preferential pairing of 8-oxo-dGTP with template dA. In Polη, when R61 was substituted with alanine, the ratio of pairing of dA to 8-oxo-dGTP compared to pairing of dC was reduced from 660:1 in wild type to 65:1 in R61A (0.79:0.0012 in wild type and 0.13:0.0020 in R61A, Table 2). Moreover, the substitution of R61 with lysine (R61K) resulted in the ratio of pairing of dA to 8-oxo-dGTP compared to pairing of dC of 7:1 (0.19:0.028 in R61K, Table 2, Figure 2). In Polκ, the Y112A mutant had less preference for incorrectly pairing 8-oxo-dGTP with template dA (Figure 1). This was primarily because the replacement of Y112 with A more severely reduced its efficiency for pairing 8-oxo-dGTP with template dA (270-fold reduction) compared to the reduction in its efficiency for pairing with template dC (15-fold reduction) (Table 1). Thus, the ratio of pairing of dA to 8-oxo-dGTP compared to pairing of dC was reduced from 11:1 to 0.6:1 by the Y112A amino acid substitution (0.026:0.0024 in wild type and 0.000096:0.00016 in Y112A, Table 1). In addition to its role as the steric gate, Y112 was previously shown to be involved in bypass DNA synthesis; e.g. pairing dCTP with template a benzo[a]pyrene diol epoxide-N^2-dG adduct and the extension of primers with terminal mismatches (31). Thus, the amino acid at the 112 position may interact with both the base and the sugar moiety of the incoming dNTPs. These data suggest that

Table 2. Steady-state kinetic parameters for C8-oxidized dNTP by wild-type Polη and R61 mutants

Template/dNTP	hPolη	k_{cat}, min^{-1}	K_m, μM^{-1}	k_{cat}/K_m, μM^{-1} min^{-1}	Related efficiency
dA/dTTP					
	WT[a]	28 ± 2.7	5.1 ± 1.4	5.4	1.0
	R61K	40 ± 5.9	17 ± 4.5	2.3	0.43
	R61A	8.0 ± 1.2	12 ± 3.5	0.7	0.13
dA/8-oxo-dGTP					
	WT	18 ± 1.8	22 ± 6.2	0.79	1.0
	R61K	21 ± 4.8	110 ± 41	0.19	0.24
	R61A	5.4 ± 1.3	42 ± 23	0.13	0.16
dC/dGTP					
	WT	11 ± 1.8	3.1 ± 1.2	3.6	1.0
	R61K	17 ± 1.2	4.6 ± 0.71	3.7	1.0
	R61A	6.3 ± 1.8	6.3 ± 3.5	1.0	0.27
dC/8-oxo-dGTP					
	WT	0.87 ± 0.21	720 ± 320	0.0012	1.0
	R61K	4.6 ± 0.58	160 ± 49	0.028	23
	R61A	0.37 ± 0.050	180 ± 56	0.0020	1.7
dG/dCTP					
	WT	33 ± 2.9	3.2 ± 87	10	1.0
	R61K	38 ± 3.3	7.4 ± 1.5	5.1	0.49
	R61A	14 ± 2.1	3.7 ± 1.7	3.7	0.35
dG/8-oxo-dATP					
	WT	0.90 ± 0.16	370 ± 150	0.0024	1.0
	R61K	0.78 ± 0.I4	510 ± 190	0.0015	0.63
	R61A	0.33 ± 0.063	180 ± 100	0.0018	0.74
dT/dATP					
	WT	18 ± 2.4	5.7 ± 1.5	3.1	1.0
	R61K	22 ± 2.8	6.8 ± 1.7	3.2	1.0
	R61A	14 ± 4.6	11 ± 5.7	1.3	0.43
dT/8-oxo-dATP					
	WT	0.56 ± 0.070	150 ± 46	0.0036	1.0
	R61K	3.2 ± 0.33	61 ± 16	0.052	14
	R61A	0.26 ± 0.016	43 ± 9.2	0.0061	1.7

[a]WT: wild-type hPolη

Y112 may stabilize the pairing of 8-oxo-dGTP with template dA in the active site of the Pol. In contrast, the F18 position of Polη, which corresponds to Y112 in Polκ, did not appear to play a role in the specificity for pairing 8-oxo-dGTP with template dA. Therefore, amino acids involved in the specificity of incorporating 8-oxo-dGTP into DNA are not conserved between Polη and Polκ, despite the fact that they belong to the same Y-family.

In Polη, the substitution of R61 with lysine elevated its preferences for pairing 8-oxo-dGTP with dC and 8-oxo-dATP with dT without affecting other activities; e.g. incorporating unaltered dNTP into DNA or bypassing oxidized dG or dA or thymine dimers in template DNA (Figure 2, Table 2, Supplementary Figure S5). These results suggested that R61 specifically inhibited the ability to correctly pair C8-oxidized dNTPs with template DNA. To investigate how R61 modulated the conformation of incoming 8-oxo-dGTP in the active site, we modeled the predicted *syn* and *anti* structures of 8-oxo-dGTP paired with dA or dC in the active site of yeast Polη. In this model, arginine 73, which corresponds to R61 of human Polη, was substituted with lysine or alanine (Figure 3). The model suggested that the side chain of arginine may constitute a steric constraint, because it would not accommodate the O^8 of an 8-oxo-dGTP in the *anti* conformation, but could accommodate it in the *syn* conformation (Figure 3A). This may be the basis for the preference shown by Polη for pairing 8-oxo-dGTP with template dA. Interestingly, when the arginine was substituted with lysine, the model indicated that the ε-amino group and O^8 of 8-oxo-dGTP in the *anti* conformation may be interacted electrostatically (Figure 3B). These results suggested that the lysine, but not arginine, might stabilize 8-oxo-dGTP in the *anti* formation; this would enhance the preference for correctly pairing 8-oxo-dGTP with template dC. In the case of alanine, the side chain did not interact with 8-oxo-dGTP (Figure 3C). Thus, the slight enhancement in the preference of R61A for pairing 8-oxo-dGTP with template dA may be due to the lack of a steric constraint of R61 in the active site of Polη. This prediction, based on model structure, could also be applicable to the preference of Polη for correctly pairing 8-oxo-dATP with template dT; the arginine may not accommodate the 8-oxo-dATP in the *anti* conformation, and the substituted lysine may induce 8-oxo-dATP to assume the *anti* conformation with the electrostatic interaction, and thus, would result in pairing with template dT. These predictions are in accordance with our biochemical findings that R61A and R61K exhibited increased preferences for pairing 8-oxo-dGTP with dC and 8-oxo-dATP with dT compared to the wild-type Polη (Table 2). Therefore, R61 appeared to play a critical role in modulating the *anti* or *syn* conformation of 8-oxo-dGTP in the active site of Polη. In human

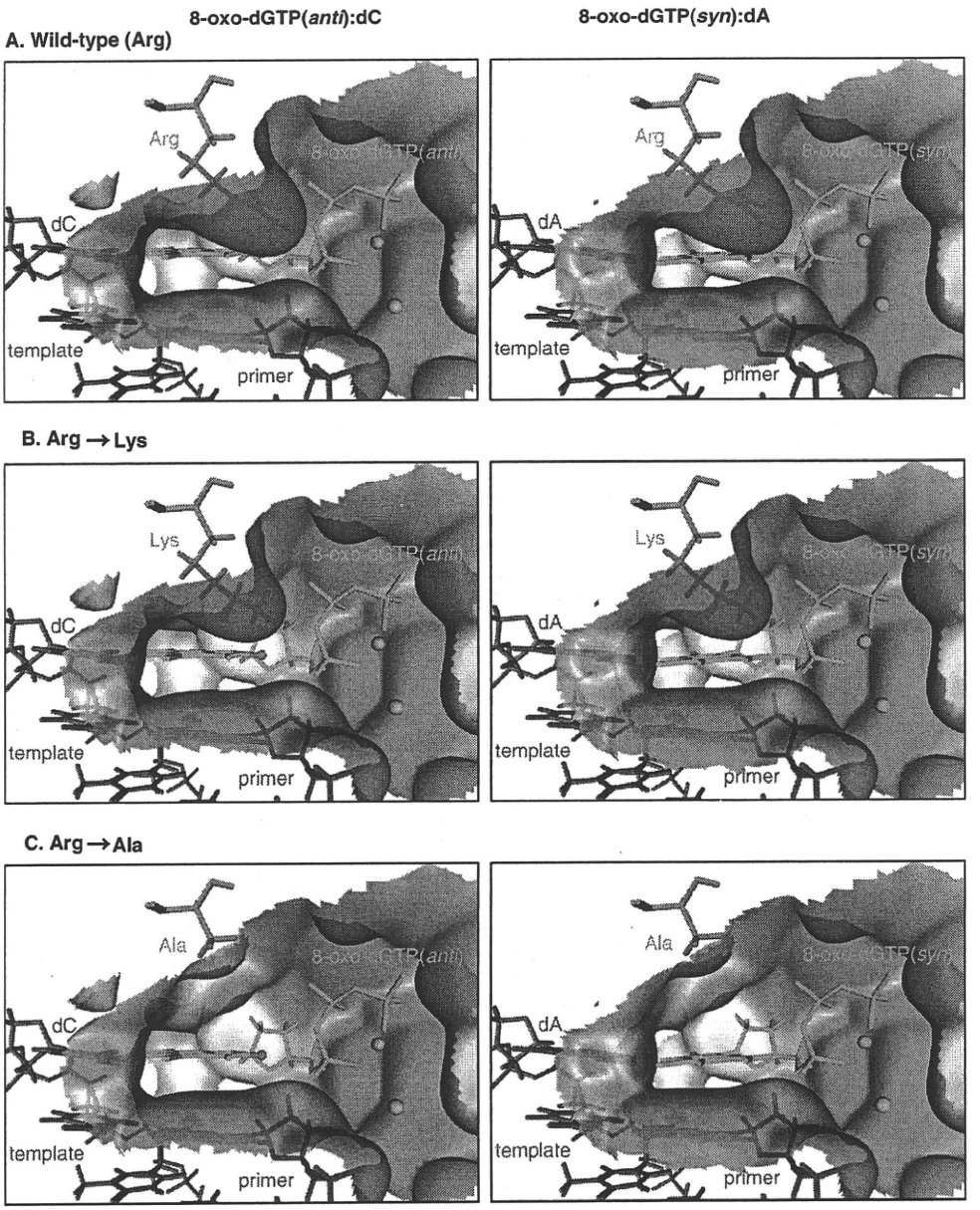

Figure 3. Molecular models of the incoming 8-oxo-dGTP in the active site of Polη. When the incoming 8-oxo-dGTP (cyan stick) forms the *anti* conformation (left panels), the side chain of arginine (displayed as a purple stick) may sterically clash with O^8 (red ball) of the incoming 8-oxo-dGTP, which may be the reason for the poor incorporation of 8-oxo-dGTP opposite template dC (green stick) (**A**). Proper pairing with template dC can be achieved, however, when arginine is substituted with lysine (**B**) or alanine (**C**) because of no steric hindrance. An electrostatic interaction between the lysine residue and O^8 of 8-oxo-dGTP may facilitate the incorporation of 8-oxo-dGTP opposite template dC (B). When the incoming 8-oxo-dGTP forms the *syn* conformation (right panels), there appear no steric or electrostatic interactions between the amino acids and O^8 of 8-oxo-dGTP (A–C). All models were constructed based on the crystal structure of yeast Polη [PDB#2R8J (21)]. The active site of Polη is displayed as Gaussian surface (colored according to its electric charge).

Polι, there is a lysine residue at the position corresponding to the R61 of Polη (Supplementary Figure S1). However, Polι always paired 8-oxo-dGTP with dA. Thus, the mechanism underlying the preference of Polη for pairing 8-oxo-dGTP with template dA may be unique to this enzyme.

Human Polβ has an asparagine in its active site, i.e. N279, that was shown to be involved in its specificity for the incorporation of oxidized dNTPs (39). Polβ was shown to preferentially pair 8-oxo-dGTP with template dA. The substitution of N279 with alanine (N279A) reduced the activity of Polβ incorporating 8-oxo-dGTP with template dA by almost 1000-fold, but it decreased the activity incorporating it with template dC by about 3-fold. Thus, the ratio of pairing of dA to 8-oxo-dGTP compared to pairing of dC was altered from 24:1

(wild-type Polβ) to 1 : 14 (N279A). It was proposed that the side chain of N279 might favorably interact with 8-oxo-dGTP in the *syn* conformation. For instance, there may be a hydrogen bond between the O^8 of 8-oxo-dGTP in the *syn* conformation and the asparagine side chain of the Pol; this would stabilize the *syn* conformation. This proposed mechanism is contrary to the mechanism we proposed here for Polη, where the side chain of R61 appeared to disturb the formation of the *anti* conformation and thus enhance the formation of the *syn* conformation. Bacteriophage ϕ29 Pol, which belongs to the B-family, has shown a preference for pairing 8-oxo-dGTP with dC over dA; thus the ratio of pairing of dA to 8-oxo-dGTP compared to pairing of dC was 3 : 1 (38). It has been shown that the lysine residue (K560) of ϕ29 Pol was involved with this specificity. Contrary to Polη, the K560 residue appeared to collide with the N^1, N^2 and O^6 atoms of 8-oxo-dGTP in the *syn* conformation, thus inducing the *anti* conformation and correct pairing activity. These results show that the amino acids that govern the specificity for the incorporation of 8-oxo-dGTP into DNA are distinct among various Pols.

Why do various Pols have different mechanisms to govern the specificity for the incorporation of oxidized dGTP? In general, replicative Pols incorporate 8-oxo-dGTP poorly and prefer to incorporate it opposite template dC as described earlier. This seems reasonable because the poor incorporation and correct specificity contribute to the genome stability. In this regard, it is understandable that the replicative Pols have effective mechanisms to exclude 8-oxo-dGTP pairing with template dA such as collision of K560 of bacteriophage ϕ29 pol with the N^1, N^2 and O^6 atoms of 8-oxo-dGTP in the *syn* conformation (38). In contrary, Polβ (X-family) and Y-family Pols incorporate 8-oxo-dGTP into DNA in relatively high efficiency and their incorporation specificity is opposite template dA rather than template dC (41). Because of their roles in DNA repair and translesion bypass, DNA synthesis may be more important (higher priority) than the fidelity. Therefore, they may incorporate dNTPs, even oxidized ones, into DNA in relatively high yield. Incorporation of 8-oxo-dGTP opposite dA may be beneficial for the cells exposed to oxidative stress. For example, pairing of 8-oxo-dGMP:dA may induce genetic diversity, which may be helpful to survive in stressful environment for Archaea and bacteria (42). The pairing may be recognized by mismatch repair proteins (43) and the recognition may induce apoptosis in mammalian cells, which eliminates cells damaged by ROS (44). Each Y-family Pol may have created its own mechanism to incorporate it opposite template dA during evolution.

In summary, human Polη and Polκ showed a preference for incorrectly pairing 8-oxo-dGTP with template dA, and this specificity appeared to be caused by the presence of distinct amino acids. The Y112 residue in Polκ may interact with the sugar and/or base of the incoming 8-oxo-dGTP, thereby forcing it to assume the *syn* conformation in the active site. The R61 residue of Polη appeared to inhibit the *anti* conformation of 8-oxo-dGTP by steric and/or electrostatic hindrance between the O^8 of 8-oxo-dGTP and the side chain of R61. These key amino acids had distinct positions in the active sites, but both were involved in inducing the *anti* conformation of 8-oxo-dGTP. Thus, we proposed that two Y-family Pols, human Polη and Polκ, employed different mechanisms for achieving the same specificity for incorporating oxidized dNTPs into DNA. The efficiency and specificity of Polη and Polκ for pairing 8-oxo-dGTP with template dA during DNA synthesis may lead to transversions of A to C. We are currently investigating this hypothesis with human cells in our laboratory.

SUPPLEMENTARY DATA

Supplementary Data are available at NAR Online.

ACKNOWLEDGEMENTS

We thank Dr Hiroyuki Kamiya at Hokkaido University for the generous gift of 2-OH-dATP.

FUNDING

Funding for open access charge: The Ministry of Education, Culture, Sports, Science and Technology, Japan (MEXT, 18201010); Ministry of Health, Labor and Welfare, Japan (H21-Food-General-009); Japan Health Science Foundation (KHB1007).

Conflict of interest statement. None declared.

REFERENCES

1. Friedberg,E.C. (2003) DNA damage and repair. *Nature*, **421**, 436–440.
2. Friedberg,E.C., Walker,G.C., Siede,W., Wood,R.D., Schultz,R.A. and Ellenberger,T. (2006) *DNA Repair and Mutagenesis*, 2nd edn. ASM Press, Washington, DC.
3. Lindahl,T. (1993) Instability and decay of the primary structure of DNA. *Nature*, **362**, 709–715.
4. Ames,B.N. (1983) Dietary carcinogens and anticarcinogens. Oxygen radicals and degenerative diseases. *Science*, **221**, 1256–1264.
5. Feig,D.I., Reid,T.M. and Loeb,L.A. (1994) Reactive oxygen species in tumorigenesis. *Cancer Res.*, **54**, 1890s–1894s.
6. Tsuzuki,T., Nakatsu,Y. and Nakabeppu,Y. (2007) Significance of error-avoiding mechanisms for oxidative DNA damage in carcinogenesis. *Cancer Sci.*, **98**, 465–470.
7. Nakabeppu,Y., Sakumi,K., Sakamoto,K., Tsuchimoto,D., Tsuzuki,T. and Nakatsu,Y. (2006) Mutagenesis and carcinogenesis caused by the oxidation of nucleic acids. *Biol. Chem.*, **387**, 373–379.
8. Tajiri,T., Maki,H. and Sekiguchi,M. (1995) Functional cooperation of MutT, MutM and MutY proteins in preventing mutations caused by spontaneous oxidation of guanine nucleotide in *Escherichia coli*. *Mutat. Res.*, **336**, 257–267.
9. Maki,H. and Sekiguchi,M. (1992) MutT protein specifically hydrolyses a potent mutagenic substrate for DNA synthesis. *Nature*, **355**, 273–275.
10. Yanofsky,C., Cox,E.C. and Horn,V. (1966) The unusual mutagenic specificity of an *E. coli* mutator gene. *Proc. Natl Acad. Sci. USA*, **55**, 274–281.
11. Kamiya,H., Iida,E., Murata-Kamiya,N., Yamamoto,Y., Miki,T. and Harashima,H. (2003) Suppression of spontaneous and hydrogen peroxide-induced mutations by a MutT-type nucleotide pool sanitization enzyme, the *Escherichia coli* Orf135 protein. *Genes Cells*, **8**, 941–950.

12. Kamiya,H., Murata-Kamiya,N., Iida,E. and Harashima,H. (2001) Hydrolysis of oxidized nucleotides by the *Escherichia coli* Orf135 protein. *Biochem. Biophys. Res. Commun.*, **288**, 499–502.
13. Sakai,Y., Furuichi,M., Takahashi,M., Mishima,M., Iwai,S., Shirakawa,M. and Nakabeppu,Y. (2002) A molecular basis for the selective recognition of 2-hydroxy-dATP and 8-oxo-dGTP by human MTH1. *J. Biol. Chem.*, **277**, 8579–8587.
14. Fujikawa,K., Kamiya,H., Yakushiji,H., Fujii,Y., Nakabeppu,Y. and Kasai,H. (1999) The oxidized forms of dATP are substrates for the human MutT homologue, the hMTH1 protein. *J. Biol. Chem.*, **274**, 18201–18205.
15. Colussi,C., Parlanti,E., Degan,P., Aquilina,G., Barnes,D., Macpherson,P., Karran,P., Crescenzi,M., Dogliotti,E. and Bignami,M. (2002) The mammalian mismatch repair pathway removes DNA 8-oxodGMP incorporated from the oxidized dNTP pool. *Curr. Biol.*, **12**, 912–918.
16. Russo,M.T., Blasi,M.F., Chiera,F., Fortini,P., Degan,P., Macpherson,P., Furuichi,M., Nakabeppu,Y., Karran,P., Aquilina,G. *et al.* (2004) The oxidized deoxynucleoside triphosphate pool is a significant contributor to genetic instability in mismatch repair-deficient cells. *Mol. Cell. Biol.*, **24**, 465–474.
17. Rai,P., Onder,T.T., Young,J.J., McFaline,J.L., Pang,B., Dedon,P.C. and Weinberg,R.A. (2009) Continuous elimination of oxidized nucleotides is necessary to prevent rapid onset of cellular senescence. *Proc. Natl Acad. Sci. USA*, **106**, 169–174.
18. Tsuzuki,T., Egashira,A., Igarashi,H., Iwakuma,T., Nakatsuru,Y., Tominaga,Y., Kawate,H., Nakao,K., Nakamura,K., Ide,F. *et al.* (2001) Spontaneous tumorigenesis in mice defective in the MTH1 gene encoding 8-oxo-dGTPase. *Proc. Natl Acad. Sci. USA*, **98**, 11456–11461.
19. Hah,S.S., Mundt,J.M., Kim,H.M., Sumbad,R.A., Turteltaub,K.W. and Henderson,P.T. (2007) Measurement of 7,8-dihydro-8-oxo-2'-deoxyguanosine metabolism in MCF-7 cells at low concentrations using accelerator mass spectrometry. *Proc. Natl Acad. Sci. USA*, **104**, 11203–11208.
20. Nohmi,T. (2006) Environmental stress and lesion-bypass DNA polymerases. *Annu. Rev. Microbiol.*, **60**, 231–253.
21. Shimizu,M., Gruz,P., Kamiya,H., Kim,S.R., Pisani,F.M., Masutani,C., Kanke,Y., Harashima,H., Hanaoka,F. and Nohmi,T. (2003) Erroneous incorporation of oxidized DNA precursors by Y-family DNA polymerases. *EMBO Rep.*, **4**, 269–273.
22. Yamada,M., Nunoshiba,T., Shimizu,M., Gruz,P., Kamiya,H., Harashima,H. and Nohmi,T. (2006) Involvement of Y-family DNA polymerases in mutagenesis caused by oxidized nucleotides in *Escherichia coli*. *J. Bacteriol.*, **188**, 4992–4995.
23. Shimizu,M., Gruz,P., Kamiya,H., Masutani,C., Xu,Y., Usui,Y., Sugiyama,H., Harashima,H., Hanaoka,F. and Nohmi,T. (2007) Efficient and erroneous incorporation of oxidized DNA precursors by human DNA polymerase eta. *Biochemistry*, **46**, 5515–5522.
24. Hidaka,K., Yamada,M., Kamiya,H., Masutani,C., Harashima,H., Hanaoka,F. and Nohmi,T. (2008) Specificity of mutations induced by incorporation of oxidized dNTPs into DNA by human DNA polymerase eta. *DNA Repair (Amst.)*, **7**, 497–506.
25. Satou,K., Hori,M., Kawai,K., Kasai,H., Harashima,H. and Kamiya,H. (2009) Involvement of specialized DNA polymerases in mutagenesis by 8-hydroxy-dGTP in human cells. *DNA Repair (Amst.)*, **8**, 637–642.
26. Kouchakdjian,M., Bodepudi,V., Shibutani,S., Eisenberg,M., Johnson,F., Grollman,A.P. and Patel,D.J. (1991) NMR structural studies of the ionizing radiation adduct 7-hydro-8-oxodeoxyguanosine (8-oxo-7H-dG) opposite deoxyadenosine in a DNA duplex. 8-Oxo-7H-dG(syn).dA(anti) alignment at lesion site. *Biochemistry*, **30**, 1403–1412.
27. Oda,Y., Uesugi,S., Ikehara,M., Nishimura,S., Kawase,Y., Ishikawa,H., Inoue,H. and Ohtsuka,E. (1991) NMR studies of a DNA containing 8-hydroxydeoxyguanosine. *Nucleic Acids Res.*, **19**, 1407–1412.
28. Prakash,S., Johnson,R.E. and Prakash,L. (2005) Eukaryotic translesion synthesis DNA polymerases: specificity of structure and function. *Annu. Rev. Biochem.*, **74**, 317–353.
29. Ling,H., Boudsocq,F., Woodgate,R. and Yang,W. (2001) Crystal structure of a Y-family DNA polymerase in action: a mechanism for error-prone and lesion-bypass replication. *Cell*, **107**, 91–102.
30. Alt,A., Lammens,K., Chiocchini,C., Lammens,A., Pieck,J.C., Kuch,D., Hopfner,K.P. and Carell,T. (2007) Bypass of DNA lesions generated during anticancer treatment with cisplatin by DNA polymerase eta. *Science*, **318**, 967–970.
31. Niimi,N., Sassa,A., Katafuchi,A., Gruz,P., Fujimoto,H., Bonala,R.R., Johnson,F., Ohta,T. and Nohmi,T. (2009) The steric gate amino acid tyrosine 112 is required for efficient mismatched-primer extension by human DNA polymerase kappa. *Biochemistry*, **48**, 4239–4246.
32. Anderson,H.J., Vonarx,E.J., Pastushok,L., Nakagawa,M., Katafuchi,A., Gruz,P., Di Rubbo,A., Grice,D.M., Osmond,M.J., Sakamoto,A.N. *et al.* (2008) Arabidopsis thaliana Y-family DNA polymerase eta catalyses translesion synthesis and interacts functionally with PCNA2. *Plant J.*, **55**, 895–908.
33. Trincao,J., Johnson,R.E., Escalante,C.R., Prakash,S., Prakash,L. and Aggarwal,A.K. (2001) Structure of the catalytic core of S. cerevisiae DNA polymerase eta: implications for translesion DNA synthesis. *Mol. Cell*, **8**, 417–426.
34. Lone,S., Townson,S.A., Uljon,S.N., Johnson,R.E., Brahma,A., Nair,D.T., Prakash,S., Prakash,L. and Aggarwal,A.K. (2007) Human DNA polymerase kappa encircles DNA: implications for mismatch extension and lesion bypass. *Mol. Cell*, **25**, 601–614.
35. Sekiguchi,M. and Tsuzuki,T. (2002) Oxidative nucleotide damage: consequences and prevention. *Oncogene*, **21**, 8895–8904.
36. Einolf,H.J. and Guengerich,F.P. (2001) Fidelity of nucleotide insertion at 8-oxo-7,8-dihydroguanine by mammalian DNA polymerase δ. Steady-state and pre-steady-state kinetic analysis. *J. Biol. Chem.*, **276**, 3764–3771.
37. Einolf,H.J., Schnetz-Boutaud,N. and Guengerich,F.P. (1998) Steady-state and pre-steady-state kinetic analysis of 8-oxo-7,8-dihydroguanosine triphosphate incorporation and extension by replicative and repair DNA polymerases. *Biochemistry*, **37**, 13300–13312.
38. de Vega,M. and Salas,M. (2007) A highly conserved tyrosine residue of family B DNA polymerases contributes to dictate translesion synthesis past 8-oxo-7,8-dihydro-2'-deoxyguanosine. *Nucleic Acids Res.*, **35**, 5096–5107.
39. Miller,H., Prasad,R., Wilson,S.H., Johnson,F. and Grollman,A.P. (2000) 8-oxodGTP incorporation by DNA polymerase β is modified by active-site residue Asn279. *Biochemistry*, **39**, 1029–1033.
40. Kamiya,H. and Kasai,H. (1995) Formation of 2-hydroxydeoxyadenosine triphosphate, an oxidatively damaged nucleotide, and its incorporation by DNA polymerases. Steady-state kinetics of the incorporation. *J. Biol. Chem.*, **270**, 19446–19450.
41. Nohmi,T., Kim,S.R. and Yamada,M. (2005) Modulation of oxidative mutagenesis and carcinogenesis by polymorphic forms of human DNA repair enzymes. *Mutat. Res.*, **591**, 60–73.
42. Friedberg,E.C., Wagner,R. and Radman,M. (2002) Specialized DNA polymerases, cellular survival, and the genesis of mutations. *Science*, **296**, 1627–1630.
43. Macpherson,P., Barone,F., Maga,G., Mazzei,F., Karran,P. and Bignami,M. (2005) 8-oxoguanine incorporation into DNA repeats in vitro and mismatch recognition by MutSalpha. *Nucleic Acids Res.*, **33**, 5094–5105.
44. Hardman,R.A., Afshari,C.A. and Barrett,J.C. (2001) Involvement of mammalian MLH1 in the apoptotic response to peroxide-induced oxidative stress. *Cancer Res.*, **61**, 1392–1397.

RADIATION RESEARCH 173, 138–147 (2010)
0033-7587/10 $15.00

DOI: 10.1667/RR1932.1

Radiation Dose-Rate Effect on Mutation Induction in Spleen and Liver of *gpt* delta Mice

Naohito Okudaira,[a] Yoshihiko Uehara,[a] Kazuo Fujikawa,[b] Nao Kagawa,[b] Akira Ootsuyama,[c] Toshiyuki Norimura,[c] Ken-ichi Saeki,[d] Takehiko Nohmi,[e] Ken-ichi Masumura,[e] Tsuneya Matsumoto,[f] Yoichi Oghiso,[f] Kimio Tanaka,[f] Kazuaki Ichinohe,[f] Shingo Nakamura,[f] Satoshi Tanaka[f] and Tetsuya Ono[a,1]

[a] *Department of Cell Biology, Graduate School of Medicine, Tohoku University, Sendai 980-8575, Japan;* [b] *Deparment of Life Science, Faculty of Science and Technology, Kinki University, Kowakae, Higashiosaka 577-8502, Japan;* [c] *Department of Radiation Biology and Health, University of Occupational and Environmental Health, Kitakyushu, 807-8555, Japan;* [d] *Yokohama College of Pharmacy, Totsuka-ku, Yokohama 245-0066, Japan;* [e] *Division of Genetics and Mutagenesis, National Institute of Health Sciences, Kamiyoga, Setagaya-ku, Tokyo 158-8501, Japan; and* [f] *Institute for Environmental Sciences, Rokkasho, Aomori 039-3212, Japan*

Okudaira, N., Uehara, Y., Fujikawa, K., Kagawa, N., Ootsuyama, A., Norimura, T., Saeki, K., Nohmi, T., Masumura, K., Matsumoto, T., Oghiso, Y., Tanaka, K., Ichinohe, K., Nakamura, S., Tanaka, S. and Ono, T. Radiation Dose-Rate Effect on Mutation Induction in Spleen and Liver of *gpt* delta Mice. *Radiat. Res.* 173, 138–147 (2010).

The effect of dose rate on radiation-induced mutations in two somatic tissues, the spleen and liver, was examined in transgenic *gpt* delta mice. These mice can be used for the detection of deletion-type mutations, and these are the major type of mutation induced by radiation. The dose rates examined were 920 mGy/min, 1 mGy/min and 12.5 μGy/min. In both tissues, the number of mutations increased with increasing dose at each of the three dose rates examined. The mutation induction rate was dependent on the dose rate. The mutation induction rate was higher in the spleen than in the liver at the medium dose rate but was similar in the two tissues at the high and low dose rates. The mutation induction rate in the liver did not show much change between the medium and low dose rates. Analysis of the molecular nature of the mutations indicated that 2- to 1,000-bp deletion mutations were specifically induced by radiation in both tissues after high- and low-dose-rate irradiation. The occurrence of deletion mutation without any sequence homology at the break point was elevated in spleen after high-dose-rate irradiation. The results indicate that the mutagenic effects of radiation in somatic tissues are dependent on dose rate and that there is some variability between tissues. © 2010 by Radiation Research Society

INTRODUCTION

Most radiation effects in biological systems influenced by the dose rate. Quantitative studies of the dose-rate effect are important for risk estimation as well as for understanding the mechanisms involved in radiation effects. Mutations are one of the most extensively studied biological end points, because they could be involved in long-term effects of radiation such as cancer induction, life-shortening and transgenerational effects. However, most studies have been performed using cultured cells, and studies in animal tissues have been limited to spleen lymphocytes (*1*), intestinal stem cells (*2*) and germ-line cells in gonads (*3, 4*). Mutations in germ-line cells were studied extensively by two groups working with mice (*3, 4*). They found that the efficiency of mutation induction was reduced to one-third as the dose rate decreased from 900 mGy/min to 8 mGy/min. Below 8 mGy/min, Russell *et al.* did not find any significant variation in mutation induction efficiency for dose rates down to 7 μGy/min (*4*). Lyon *et al.*, on the other hand, suggested that the efficiency of mutation induction might be elevated at 10 μGy/min compared to the dose-rate range of 50 μGy/min to 8 mGy/min, although the difference was small (*3*). A dose-rate effect in germ cells was also observed in the fish *Oryzias latipes* (*5*). Studies in somatic tissues have been performed using mice. One study involved mutations in the *Hprt* gene in splenic lymphocytes (*1*), and another study was of mutations in the *Dlb1* gene in the stem cells of the small intestine (*2*). Dose-rate effects were found in these cells, with differences between high (about 1 Gy/min) and low dose rates (0.099 mGy/min for *Hprt* and 10 mGy/min for *Dlb1*). In the *Hprt* gene in splenic lymphocytes, the efficiency of mutation induction was similar between 690 μGy/min and 99 μGy/min. Chromosomal translocations in blood lymphocytes were also reported to show similar radiosensitivities at 3.5, 14 and 28 μGy/min (*6*). Somatic cells in culture also revealed a similar dose-rate dependence [(*7, 8*) and references therein]. All of these studies found good agreement on the overall pattern of

[1] Address for correspondence: Department of Cell Biology, Graduate School of Medicine, Tohoku University, Seiryo-machi 2-1, Aoba-ku, Sendai 980-8575, Japan; e-mail: tono@mail.tains.tohoku.ac.jp.

observed dose-rate dependences: a high efficiency of mutation induction at dose rates of 0.5–2 Gy/min and low efficiencies in a dose-rate range of 3.5 μGy/min to 50 mGy/min.

To examine dose-rate effects in very low-dose-rate ranges, Valenchic and Knudson suggested that mutation induction as well as many other biological end points might be elevated in certain low-dose-rate ranges, which would make the dose-rate–response curves appear parabolic (*9, 10*). On the other hand, more recent studies on chromosomal abnormalities in splenic lymphocytes revealed a constant decline of efficiency in the dose-rate range of 890 mGy/min to 0.76 μGy/min (*11*). Thus more detailed studies on dose-rate effects are desirable, especially in different somatic tissues. The purpose of the present study was to elucidate the dose-rate effects of radiation-induced mutation in two somatic tissues, the spleen and liver.

The main problem for mutation studies in somatic tissues *in vivo* was the lack of a method to detect mutations. However, this has been overcome by the creation of transgenic mice that are suitable for mutation assays. These mice contain bacterial genes in their genome, and the bacterial genes can be assayed for mutations by using bacterial systems (*12*). In the work described here, transgenic *gpt* delta mice were used to study dose-rate effects in the spleen and liver. These mice contain lambda EG10 genomic DNA in chromosome 17, and the Spi$^-$ assay can be applied to focus exclusively on deletion-type mutations in the *red-gam* genes located in the central part of the lambda EG10 genome (*13, 14*). In previous studies, deletions were found to be the predominant type of mutation induced by radiation in the spleen and liver when a 3.1-kbp-long *lacZ* gene was used to monitor mutations (*15, 16*). Nohmi *et al.* (*17*) and Furuno-Fukushi *et al.* (*18*) reported that the *gpt* delta mice can be used to detect mutations induced by 5 to 50 Gy of radiation.

MATERIALS AND METHODS

Mice and Irradiation

Transgenic *gpt* delta mice containing lambda EG10 genomic DNA (*15*) were mated to SWR mice that contained the *Dlb1*^{b} allele (*19*), and F_1 mice were used to compare mutations in the *red-gam* gene and the *Dlb1* gene. The results of a study on the *Dlb1* gene will be reported separately. Some F_1 mice were irradiated with ^{137}Cs γ rays at dose rates of 920 mGy/min or 1 mGy/min at 2 months of age in the University of Occupational and Environmental Health and were killed humanely 1 week after the end of the irradiation. Spleen and liver were excised, frozen on dry ice and kept at –70°C until use. Other F_1 mice were irradiated with a very low dose rate of 12.5 μGy/min for 483 consecutive days using a low-dose-rate irradiation facility at the Institute for Environmental Sciences. The exposures were started at 2 months of age, and the mice were exposed for 22 h every day. The remaining 2 h (10:00 am to 12:00 noon) were spent checking the health of the mice, changing food, water and cages, and cleaning the room. Control mice were treated in the same way without irradiation in a neighboring room. The mice were sampled 1 week after the end of irradiation. Spleens and livers were excised, frozen on dry ice, and kept at –70°C until use. All mice were kept under SPF conditions (*20, 21*). All procedures were conducted under the Guidelines for Animal Experiments of the University of Occupational and Environmental Health and the Institute for Environmental Sciences.

TABLE 1
Common Alterations Found in *gpt* delta Mice

Location	Alteration[a]
19,377	TTACC → TTGCC
19,787	CCGC → CC(T)GC (+1)
20,705	CTGCT → CTACT
23,118	GTTTC → GTCTC
23,849	GTGAA → GTAAA
24,068	TCATC → TCTTC
34,896	CACC → CA(A)CC (+1)
35,010	CAGAC → CAAAC
38,668	CAGTG → CAATG
39,732	GGAAA → GGGAA

[a] Base substitutions are underlined and the inserted bases are shown in parentheses. +1 indicates one base insertion.

Mutation Assays

Genomic DNA was extracted from spleens and livers using phenol. Lambda EG10 DNA integrated in the mouse genome was retrieved in the form of a phage by mixing the genomic DNA with a packaging extract (Transpack® Packaging Extract, Stratagene, La Jolla, CA) according to the manufacturer's instructions. The recovered phage was assayed by plaque formation using *E. coli* XL-1 Blue MRA. The phages containing mutations in the *red-gam* genes in the lambda phage were detected as plaques on P2-lysogenic E. coli XL-1 Blue MRA (P2) as described previously (*13, 14*).

DNA Sequence Analysis

Nucleotide sequences of the mutant phage DNA were determined with PCR amplification and sequencing of the amplified fragments. First, the 1.8-kbp *red-gam* gene was amplified with PCR. When the PCR product was obtained, it was sequenced from both ends of the fragment. When a PCR product was not produced, it was assumed that one of the PCR primer sites was deleted, and extended PCR amplification to the flanking regions using different primers was performed. The primers were chosen from nearby adjacent locations, and appropriate primers were sought by continuously testing primers sequentially from nearby locations. When PCR successfully produced a DNA fragment, it was sequenced to determine the end of the deletion mutation. The primers and their locations have been described previously (*14*). The sequences obtained were compared to those in wild-type lambda EG10.

From the sequence analyses, alterations in 10 locations in and around the *red-gam* gene were found. Since these 10 alterations were common in more than four wild-type lambda EG10 phage isolated from the mice, it was concluded that these alterations were inherent in the lambda EG10 sequence in the *gpt* delta mice used. They are listed in Table 1. All of the other alterations found were unique to mutant phage and were not found in at least three wild-type clones. They were counted as mutations. When unusual mutations were found, such as tandem, multiple or complex mutations, the alterations were confirmed by sequencing both the upper and lower DNA strands.

In one mutant clone, there was an insertion of a part of the lambda EG10 sequence in the *red-gam* gene. To determine whether the inserted sequence was produced by duplication of the original sequence or by translocation of DNA fragment, the presence of the original sequence was examined by PCR amplification using the